PKA and Sch9 Control a Molecular Switch Important for the Proper Adaptation to Nutrient Availability.

Johnny Roosen[1], Kristof Engelen[2], Kathleen Marchal[2], Janick Mathys[2], Gerard Griffioen[3+], Elisabetta Cameroni[4], Johan M. Thevelein[3], Claudio De Virgilio[4], Bart De Moor[2] and Joris Winderickx[1*]

[1]Functional Biology, [2]Department of Electrical Engineering/ESAT-SISTA and [3]Departement Moleculaire Microbiologie-VIB, Katholieke Universiteit Leuven, Kasteelpark Arenberg, B-3001 Leuven-Heverlee, Belgium. [4]Département de Biochimie Médicale, CMU, University of Geneva, CH-1211 Genève 4, Switzerland.

[+]Present address, Remynd, Minderbroederstraat 12, 3000 Leuven, Belgium

*To whom correspondence should be addressed. E-mail: joris.winderickx@bio.kuleuven.ac.be

Running Title: cAMP-gating in yeast

Key Words: cAMP-gating, Sch9/PKB, PKA, Rim15, PDS/STRE, cDNA array

Experimental Procedures: 1493 words

Summary (171), Introduction (850), Results (5071) and Discussion (2257): 8349 words

Correspondent Footnote: Corresponding author: Joris Winderickx

Functional Biology, K.U.Leuven, Kasteelpark Arenberg 31, B-3001 Heverlee-Leuven

Tel: (+) 32-16-321502 Fax: (+) 32-16-321967

Joris.winderickx@bio.kuleuven.ac.be

Summary

In the yeast *Saccharomyces cerevisiae*, PKA and Sch9, exert similar physiological roles in response to nutrient availability. However, their functional redundancy complicates to distinguish properly the target genes for both kinases. In this paper, we analysed different phenotypic read-outs. The data unequivocally showed that both kinases act through separate signalling cascades. In addition, genome-wide expression analysis under conditions and with strains in which either PKA and/or Sch9 signalling was specifically affected, demonstrated that both kinases synergistically or oppositely regulate given gene targets. Unlike PKA, which negatively regulates STRE- and PDS-driven gene expression, Sch9 appears to exert additional positive control on the Rim15-effector Gis1 to regulate PDS-driven gene expression. The data presented are consistent with a cAMP-gating phenomenon recognized in higher eukaryotes consisting of a main gatekeeper, the protein kinase PKA, switching on or off the activities and signals transmitted through primary pathways such as, in case of yeast, the Sch9-controlled signaling route. This mechanism allows fine-tuning various nutritional responses in yeast cells, allowing them to adapt metabolism and growth appropriately.

Introduction

For the yeast *Saccharomyces cerevisiae* nutrients are the prime environmental factors controlling growth, proliferation and metabolism. For instance, the addition of glucose to respiring cells triggers the necessary adaptations that reset metabolism to fermentation (Jiang *et al.*, 1998). One of the key signalling cascades involved in this process is the Ras/cAMP pathway. Addition of fermentable sugars triggers activation of adenylate cyclase and the production of a pronounced cAMP spike (Mbonyi *et al.*, 1988). Cyclic AMP in turn activates PKA by binding to the two *BCY1*-encoded regulatory subunits allowing their dissociation from the two catalytic subunits, which are encoded by one of three partially redundant *TPK* genes (*i.e. TPK1*, *TPK2* and *TPK3*) (Toda *et al.*, 1987a; Toda *et al.*, 1987b; Doskeland *et al.*, 1993). Cyclic AMP is quickly degraded by the low and high affinity phosphodiesterases Pde1 and Pde2 (Nikawa *et al.*, 1987b; Wilson and Tatchell, 1988). Furthermore, glucose-induced activation of the Ras/cAMP pathway is strictly controlled through negative feedback mechanisms (Nikawa *et al.*, 1987a; Ma *et al.*, 1999). Consequently, activation of cAMP synthesis beyond the basal level is a transient effect, limited to the short period of the onset of fermentation. Glucose-induced activation of PKA has been reported to trigger additional adaptations associated with optimal growth conditions, like the mobilization of reserve carbohydrates and the reduction of the overall stress resistance (Thevelein *et al.*, 2000). Some of these physiological effects appear by changes in enzyme activities. Fairly well established examples are phosphofructokinase 2, the low-affinity phosphodiesterase and the trehalose-degrading enzyme trehalase (Ortiz *et al.*, 1983; Uno *et al.*, 1983; Francois *et al.*, 1984; Thevelein and Beullens, 1985; Zahringer *et al.*, 1998). Other PKA-mediated effects can be accounted for by changes in transcription. For instance, PKA has been shown to modulate the activity of the multifunctional transcription factor Rap1 for the induction of ribosomal protein

genes (Klein and Struhl, 1994). In addition, PKA counteracts the general stress response by compromising nuclear translocation of the partially redundant zinc-finger transcription factors, Msn2 and Msn4 (Gorner *et al.*, 1998; Garreau *et al.*, 2000). These factors bind to stress-responsive elements (STRE) in the promoter of many genes such as *HSP12*, *CTT1* and genes encoding different subunits of the trehalose synthase complex (Marchler *et al.*, 1993; Ruis and Schuller, 1995; Winderickx *et al.*, 1996; Boy-Marcotte *et al.*, 1998; Moskvina *et al.*, 1998). Expression of stress responsive genes also largely depends on Rim15, a protein kinase immediately downstream of and negatively regulated by PKA (Reinders *et al.*, 1998; Pedruzzi *et al.*, 2000). Consistently, deletion of *MSN2* and *MSN4* or *RIM15* can suppress the lethality of mutants with compromised PKA activity (Reinders *et al.*, 1998; Smith *et al.*, 1998). Rim15 appears to be specifically required for proper entry into stationary phase by inducing typical G_0 traits such as accumulation of glycogen, trehalose and Gis1-dependent PDS-element (post-diauxic shift) driven gene expression (Reinders *et al.*, 1998; Pedruzzi *et al.*, 2000). Interestingly, Msn2/4 and Gis1 cooperatively mediate almost the entire Rim15-dependent transcriptional response at the diauxic shift (Cameroni *et al.*, 2004).

The protein kinase Sch9 is structurally related to the catalytic subunits of PKA. It was initially isolated as a high-copy suppressor of the growth defect resulting from disruption of PKA signalling (*e.g.* following loss of Ras or PKA activity) (Toda *et al.*, 1988). Conversely, the slow growth phenotype associated with loss of Sch9 can be suppressed by enhanced PKA activity, suggesting that both kinases may act, at least in part, redundantly or that overexpression of one kinase compensates for the loss of function of the other via promiscuous phosphorylation (Toda *et al.*, 1988). More recently, Sch9 has been implemented in the Fermentable Growth Medium-induced (FGM) pathway as a glucose- and nitrogen-responsive regulator that acts independently of cAMP to control phenotypic characteristics known to be affected by PKA such as stress

88 resistance (Crauwels *et al.*, 1997; Thevelein and de Winde, 1999 and references therein).
89 However, the precise relationship between PKA and Sch9 has not been established yet as it was
90 not unambiguously demonstrated whether Sch9 functions in parallel to the Ras/cAMP pathway.
91 Furthermore, Sch9 is also involved in the regulation of cell size (Jorgensen *et al.*, 2002) and
92 longevity (Fabrizio *et al.*, 2001; Fabrizio *et al.*, 2003). Although several putative substrates have
93 been identified for PKA, none have been described for Sch9. Some candidate substrates were
94 identified for both kinases with overlapping substrate specificities (Zhu *et al.*, 2000).
95 Furthermore, given their functional redundancy, it is difficult to differentiate properly between
96 specific target genes.

97 This study further addresses the relationship between PKA and Sch9 at the transcriptional
98 level. Results are presented demonstrating that PKA and Sch9 are key elements of separate
99 signalling cascades. Our data point to a Sch9- and Rim15-dependent molecular switch involving
100 Gis1 and Msn2/4 to control STRE- and PDS-driven gene expression. As Rim15 is negatively
101 regulated by PKA on glucose medium, its role is to reset the molecular switch as a function of
102 PKA activity and the available carbon source. This mechanism closely resembles a phenomenon
103 known as cAMP-gating in higher eukaryotes in which PKA modulates the signal flow through
104 primary pathways (Iyengar, 1996; Jordan and Iyengar, 1998).

Results

Sch9 contributes nutritional information independently of PKA.

In order to elucidate in more detail the functional relationship between PKA and Sch9, we initially introduced the deletion of *SCH9* in the *tpk1*Δ *tpk2*Δ *tpk3*Δ *msn2*Δ *msn4*Δ strain that lacks PKA activity but is able to grow because of the suppressive effect obtained by deletion of the two STRE-binding transcription factors Msn2 and Msn4 (Smith *et al.*, 1998). However, the deletion of *SCH9* in this background caused growth failure (data not shown), which is consistent with the previous observations that Sch9 is essential in strains with reduced activity of the Ras/cAMP pathway (Lorenz *et al.*, 2000). Therefore, we shifted strategy and constructed a strain where the activity of PKA is specifically dependent on the addition of extracellular cAMP. To this end, the genes *PDE2* and *CYR1,* encoding respectively the high affinity cAMP phosphodiesterase and adenylate cyclase, were deleted in a W303-1A wild type. As reported, the lack of Pde2 makes the cells responsive to extracellular cAMP (Mitsuzawa, 1993; Wilson *et al.*, 1993) and permits to bypass the lethality caused by loss of Cyr1 (Fig. 1A). Hence, such a strain grows solely on cAMP-containing medium. Similar to the alleviation of the growth defect of the PKA-deficient mutant described above, the loss of the highly redundant transcription factors Msn2 and Msn4 or the overexpression of Sch9 allows the *pde2Δ cyr1Δ* mutant to grow in the absence of cAMP, albeit to different extents. Note that addition of cAMP or the additional deletion of *MSN2* and *MSN4* in the *pde2Δ cyr1Δ* mutant supported solely fermentative growth whereas enhanced Sch9 activity supported respiratory growth as well.

Fig. 1

Next, we introduced the deletion of *SCH9* in the quadruple *pde2Δ cyr1Δ msn2Δ msn4Δ* mutant and found that loss of Sch9 abolished the ability of the corresponding mutant to grow fermentatively on glucose in the absence of cAMP (Fig. 1A). This is again consistent with the observations that the deletion of *SCH9* is essential in strains with reduced activity of PKA or the Ras/cAMP pathway (Kraakman *et al.*, 1999; Lorenz *et al*., 2000). However, although the quintuple *pde2Δ cyr1Δ msn2Δ msn4Δ sch9Δ* mutant did not grow in the absence of cAMP, the strain retained its viability after cAMP starvation for up to 24h and it responded to the re-addition of cAMP by resumption of growth (data not shown). Interestingly, we also noticed that even in the presence of cAMP, the *pde2Δ cyr1Δ msn2Δ msn4Δ sch9Δ* mutant still displays a severe growth defect on minimal glucose-containing medium (supplementary data in Fig. S1A) and this phenotype could only be restored by reintroduction of *SCH9* and not by overexpression of *TPK1* or *BCY1* (supplementary data in Fig. S1B). These data are consistent with Sch9 being important for transmitting additional nutritional signals besides those generated by the presence of a fermentable carbon source (Thevelein and de Winde, 1999). Also the overexpression of *SCH9* in the quadruple *pde2Δ cyr1Δ msn2Δ msn4Δ* mutant indicated that cAMP-activated PKA cannot compensate for all functions of Sch9 because enhanced Sch9 activity improved growth on glycerol-containing media independently of cAMP. In summary, our data indicate that Sch9 controls more growth regulatory functions than those regulated by cAMP-activated PKA or Msn2/4 and hence, they favour a model in which Sch9 and PKA control partially overlapping signalling networks. Consequently, at least one of the Sch9-effector branches should converge on a component downstream of PKA while others function in parallel as illustrated in Fig. 1B.

PKA is required but not sufficient for proper glucose-induced trehalase activation.

The glucose-induced activation of the trehalose degrading enzyme trehalase is one of the best-established examples in which yeast PKA has an important regulatory function (Uno *et al.*, 1983; Zahringer *et al.*, 1998). We monitored glucose-induced trehalase activation in the different strains constructed above under conditions with or without pre-treatment with 0.5 mM cAMP. As shown in Fig. 1C, addition of 100mM glucose did not induce trehalase activation in the *pde2Δ cyr1Δ msn2Δ msn4Δ* or *pde2Δ cyr1Δ msn2Δ msn4Δ sch9Δ* strains in the absence of cAMP. Also the supplementation of 0.5 mM cAMP (data points –20, -10, 0 in Fig. 1C) failed to trigger activation of trehalase although it elevated the basal activity. Only the combined treatment, i.e. addition of glucose to cAMP-treated cells, triggered a fast increase in trehalase activity but solely in the quadruple *pde2Δ cyr1Δ msn2Δ msn4Δ* mutant and not in the quintuple *pde2Δ cyr1Δ msn2Δ msn4Δ sch9Δ* mutant. The very modest increase in trehalase activity that was still present in the quintuple mutant resulted entirely from the cAMP treatment since it was also observed when only cAMP was given without a subsequent addition of glucose (results not shown). Thus, it can be concluded that cAMP-induced activation of PKA is required but not sufficient to mediate the glucose-dependent change in trehalase activity and that an additional requirement depends on Sch9. The overexpression of *SCH9* in the *pde2Δ cyr1Δ msn2Δ msn4Δ* strain, on the other hand, not only increased dramatically the basal trehalase activity but it also rendered the glucose-induced trehalase activation independent of cAMP. This confirms that over-activation of Sch9 indeed compensates for the loss of PKA activity. These data are consistent with the results obtained for growth as they show different but converging functions of Sch9 and PKA.

Identification of target genes for cAMP-activated PKA and Sch9 using genome-wide expression analysis.

In order to identify target genes controlled by cAMP-activated PKA and Sch9, we performed a genome-wide expression analysis with the strains *pde2Δ cyr1Δ msn2Δ msn4Δ*, *pde2Δ cyr1Δ msn2Δ msn4Δ sch9Δ* and *pde2Δ cyr1Δ msn2Δ msn4Δ* YIp*SCH9* that did or did not receive 3 mM cAMP after a 6-hour cAMP starvation period on galactose-containing medium. As mentioned, all strains remained viable upon cAMP starvation and responded to the re-addition of cAMP by resumption of growth (data not shown). Using these conditions, we retrieved a limited number of genes that are predominantly regulated by either PKA or Sch9 and a larger number of genes that are controlled by both kinases, as described in more detail below. The validity of the genome-wide expression data was confirmed by conventional Northern blot analysis for several randomly selected genes starting from RNA samples prepared independently of those used for the genome-wide expression analysis (see supplementary data in Fig. S2). In addition, many genes known to be affected by PKA, such as ribosomal protein (rp) genes and genes involved in reserve carbohydrate metabolism and the stress response were consistently retrieved in our analysis (Marchler *et al.*, 1993; Griffioen *et al.*, 1994; Klein and Struhl, 1994; Winderickx *et al.*, 1996; Boy-Marcotte *et al.*, 1998) (and supplementary data in Table S1). Furthermore, there is a significant overlap in the genes retrieved by our micro-array analysis and those identified by genome-wide expression analyses of glucose-induced effects in *tpk* attenuated strains and strains with overexpression of *RAS2* and *GPA2* (Wang *et al.*, 2004).

It should be noted that the results obtained for the expression of genes in the strain with overexpression of *SCH9* are difficult to interpret. Similarly to the activation of trehalase, the increase in Sch9 activity rendered many of the genes unresponsive to cAMP. Although consistent

with observations that overexpression of Sch9 compensates for the loss of PKA, one cannot rule out the possibility that this effect is simply due to aberrant phosphorylation of proteins at epitopes that in wild type cells are normally not a substrate of the Sch9 kinase. Therefore, this strain was not taken into account for the interpretation of PKA- and Sch9-mediated transcriptional effects.

Specific target genes of cAMP-activated PKA and Sch9

In order to retrieve those genes that can be considered as specific targets for either cAMP-activated PKA or Sch9, i.e. genes of which transcription predominantly depends on only one of the kinases, we applied the following selection procedure. Genes were deemed PKA specific when their fold change difference in expression exceeded 2.0 due to addition of cAMP to the strains *pde2Δ cyr1Δ msn2Δ msn4Δ* and *pde2Δ cyr1Δ msn2Δ msn4Δ sch9Δ* and of which the fold change difference due to deletion of *SCH9* was lower than 1.5, i.e. the comparisons '*pde2Δ cyr1Δ msn2Δ msn4Δ* without cAMP' versus '*pde2Δ cyr1Δ msn2Δ msn4Δ sch9Δ* without cAMP' and '*pde2Δ cyr1Δ msn2Δ msn4Δ* with cAMP' versus '*pde2Δ cyr1Δ msn2Δ msn4Δ sch9Δ* with cAMP'. This selection procedure thus retrieves those genes of which the expression is changed significantly due to the addition of cAMP irrespective of the presence of Sch9 but of which the expression does not change significantly by deletion of *SCH9* irrespective of the absence or presence of cAMP. Conversely, genes were deemed Sch9 specific when their fold change difference in expression exceeded 2.0 in the comparisons '*pde2Δ cyr1Δ msn2Δ msn4Δ* without cAMP' versus '*pde2Δ cyr1Δ msn2Δ msn4Δ sch9Δ* without cAMP' and '*pde2Δ cyr1Δ msn2Δ msn4Δ* with cAMP' versus '*pde2Δ cyr1Δ msn2Δ msn4Δ sch9Δ* with cAMP' and of which the fold change difference due to addition of cAMP in both strains was lower than 1.5. This selection procedure thus retrieves those genes of which the expression is changed significantly due to the

Table 1

deletion of *SCH9* irrespective of the absence or presence of cAMP but of which the expression does not change significantly by addition of cAMP (Table 1). Note that the fold change cut-off values were statistically determined and that they correspond to the values that allow for selection of differentially expressed genes with a confidence level of 99% or for genes of which the expression was largely unchanged with a confidence level of 90%. In this way, we identified eleven genes for which the transcription was predominantly regulated by cAMP-activated PKA and largely independent of Sch9 with functions in cell cycle and DNA processing (*NOP7*, *HCA4* and *HAS1*) and stress response (*HSP26* and *THI4*) (Table 1). Twenty-four genes were retrieved of which transcription was predominantly controlled by Sch9 and largely independent of cAMP-activated PKA (Table 1). These genes mostly play central roles in amino acid biosynthesis such as *ARO4*, *ASN2*, *BAP3*, *GLY1*, *ILV2*, *MET3*, *MET6*, *MET10* and *MET17* and other metabolic pathways such as glycolysis and gluconeogenesis (*PYC2*, *PFK1* and *SDH1*)

Expression profiling reveals synergistic and opposing effects of PKA and Sch9 on transcription of common target genes Fig.2

We applied the AQBC clustering algorithm (De Smet *et al.*, 2002) to compare and cluster the expression profiles of all the genes that responded significantly to changes in the activity of both PKA and Sch9. This allowed sorting of 918 genes into 14 different clusters (Fig. 2A). These clusters could be further classified into 5 major classes when only the first four conditions were taken into consideration*, i.e*. expression in the *pde2Δ cyr1Δ msn2Δ msn4Δ* (1) and the *pde2Δ cyr1Δ msn2Δ msn4Δ sch9Δ* (2) mutants in the absence (a) or presence (b) of cAMP. The different classes were determined based on the effect triggered by the addition of cAMP (condition 1a versus 1b and condition 2a versus 2b in Fig2A) combined with the effect obtained for the deletion

of *SCH9* (condition 1a versus 2a and condition 1b versus 2b in Fig. 2A). Thus, the subclusters in each class differed mainly in the expression profiles obtained with overexpression of *SCH9* (condition 3a and 3b in Fig. 2A), which, as mentioned, were difficult to interpret and not used in further descriptions. As deduced from the MIPS functional categories (Munich Information centre for Protein Sequences), many of the genes within each cluster encoded proteins that are involved in the same physiological or metabolic process (Fig. 2B).

To get more insight in the transcriptional mechanisms governed by PKA and Sch9, we then searched for the presence of overrepresented motifs using the genome-wide screening program REDUCE (Bussemaker *et al.*, 2001) and Motif Finder (Thijs *et al.*, 2002). In this way, we identified 14 putative *cis*-acting DNA-elements that may contribute to PKA- and/or Sch9-dependent regulation of expression (Table 2). Subsequently, we screened each element against the Transfac database (Heinemeyer *et al.*, 1998) to identify corresponding DNA-binding proteins. The different classes are described in detail below. Table 2

Class 1 contains three clusters which are enriched for genes that encode proteins with a function in translation and protein synthesis. These include ribosomal protein genes (*RPL* and *RPS* genes), translation initiation and elongation factors (e.g.: *HYP2*, *GCD11*, *EFB1*, *EFT2*…), tRNA synthetases (e.g.: *ILS1*, *GRS1*…), proteins involved in rRNA transcription (e.g.: *NHP2*, *DBP3*…), nucleotide metabolism (e.g.: *IMD2-4*, *URA7*, *URA5*, *PRS1*, *PRS3*…) and amino acid metabolism (e.g.: *AGP1*, *BAP3*…). These genes are not only induced by addition of cAMP-activated PKA but they are also positively regulated by the Sch9 protein kinase, independently of cAMP because deletion of *SCH9* dramatically reduces their expression. In agreement with previously reported data (Griffioen *et al.*, 1996; Crauwels *et al.*, 1997), the effects triggered by PKA and Sch9 appeared to be largely independent of each other (compare condition 1a versus 2a and 1b versus 2b in Fig. 2A). REDUCE and Motif Finder identified three known DNA elements,

263 i.e. RPG, RRPE and PAC and three unknown DNA elements, designated U1-U3, in genes of
264 class 1 and more in particular those of cluster 1(Table 2, Table S2) (Tavazoie *et al.*, 1999).
265 REDUCE also assigned positive F-scores for both PKA and Sch9 indicating a positive correlation
266 between transcriptional regulation through these elements and enhanced PKA and Sch9 activity
267 (Table 2). For the known elements, the RPG box was reported to be bound by Rap1, a PKA-
268 dependent multifunctional transcription factor required for expression regulation of ribosomal
269 protein (rp) genes (Griffioen *et al.*, 1994; Klein and Struhl, 1994). The RPPE (rRNA Processing
270 Element) (Tavazoie *et al.*, 1999; Hughes *et al.*, 2000) and the PAC (P and C box) elements
271 (Dequard-Chablat *et al.*, 1991) are putative recruitment sites for the histone deacetylase Rpd3,
272 which reverses histone H4 acetylation in response to nutrient limitation thereby causing
273 repression of rp genes and genes encoding proteins involved in rRNA and tRNA synthesis
274 (Kurdistani *et al.*, 2002; Rohde and Cardenas, 2003). Very recently, PKA was described to
275 negatively influence the histone deacetylase HDAC8, the mammalian homolog of yeast Rpd3,
276 through phosphorylation (Lee *et al.*, 2004). Since so far, however, no data are available for the
277 involvement of PKA or Sch9 in histone acetylation and deacetylation in yeast, we confirmed the Fig. 3
278 mathematical calculations of REDUCE by *in vivo* beta-galactosidase activity measurements using
279 a minimal promoter construct containing one single RRPE-element. As shown, both PKA and
280 Sch9 were indeed required to obtain maximal induction of the β-GAL reporter (Fig. 3A).
281 REDUCE also identified a fourth unknown DNA element, designated U4, which based on the
282 calculations should have no correlation with PKA but a positive correlation with Sch9 (Table 2).
283 Also this could be confirmed *in vivo* using a U4-driven β-GAL reporter construct (Fig. 3B). Thus,
284 although the physiological relevance of the U4 motif remains unclear, this DNA element might
285 be considered a prime candidate for Sch9-specific signalling in the control of cluster 1 genes.

Taken together, both PKA and Sch9 positively and synergistically control transcription of class 1 genes presumably through separate yet unidentified mechanisms (Fig. 2B). Our data suggest that this may involve modulation of Rap1 activity or histone deacetylase activity.

Class 2 contains three clusters that are enriched for genes encoding proteins required for the general stress response (e.g.: *SSA3*, *HSP12*, *GRE1*, *CTT1*, …), cell growth, (e.g.: *TPD3*, *ABP1*, *ARP2*…), detoxification (e.g.: *SOD2*, *CCP1*, *GPX1*, *GPX2*…), proteolysis (e.g.: *RPN5*, *RPN8*, *RPN12*, *RPT2*, *RPT4*…), reserve carbohydrate metabolism (e.g.: *TPS1*, *TSL1*, *PPG1*, *GLC3*…), the TCA cycle (e.g.: *SDH2*, *ACO1*, *KGD2*…), amino acid metabolism (e.g.: *HIS5*, *SER1*, *GDH3*…) and carbohydrate metabolism (e.g.; *GLK1*, *HXT5*, *MLS1*, *PDA1*, *PDC6*…). These genes are all repressed by cAMP-activated PKA (compare condition 1a versus 1b and 2a versus 2b in Fig. 2A), which is consistent with previously published data (Belazzi *et al.*, 1991; Werner-Washburne *et al.*, 1993; Mager and De Kruijff, 1995; Winderickx *et al.*, 1996; Boy-Marcotte *et al.*, 1998). Sch9, on the other hand, exerts a positive effect on these genes in the absence of cAMP because its deletion reduces their expression although not to the same extent as cAMP-activated PKA does (compare condition 1a versus 2a in Fig. 2A). Interestingly, however, the lack of Sch9 prevented to some extend the repression by cAMP-activated PKA for most genes, i.e. cluster 4 and 6 (compare condition 2a versus 2b in Fig. 2A). This apparent dual function of Sch9 has been noticed before, when deletion of the kinase was described to induce a high PKA-phenotype in derepressed cells while compromising maintenance of high PKA-phenotypes in repressed cells (Crauwels *et al.*, 1997). REDUCE identified the STRE (stress responsive element) and PDS (post-diauxic shift) elements which are significantly enriched in Class 2 genes (Table 2). Consistent with the literature (Marchler *et al.*, 1993; Pedruzzi *et al.*, 2000), both elements scored negative F-values and hence negatively correlated with cAMP-activated PKA, indicating that PKA mediated repression through these elements. For Sch9, there

was no strict correlation with the STRE-element while a positively correlation was found with the PDS-element. The latter was not only consistent with the marked drop in expression of the PDS-controlled genes upon activation of PKA or deletion of *SCH9* (Figure 2 and Table 3) but it was also in line with the β-galactosidase studies using a PDS reporter construct (Fig. 3C). Thus, class 2 genes are negatively regulated by cAMP-activated PKA and positively controlled by Sch9. How both kinases independently and oppositely influence expression of the genes in class 2 is described in more detail in the section below. Table 3

Class 3 contains four clusters with genes that encode proteins with a function in glycolysis and gluconeogenesis (e.g.: *ENO2*, *TDH2*, *FBA1*…), transcription regulation (*GCN4*, *ADA2*), utilization of alternative carbon sources (e.g.: *GAL1*, *GAL7*, *GAL10*…), respiration, mitochondrial biogenesis and mitochondrial transport (e.g.: *QCR9*, *MRS5*, *IMG2*, *TOM37*, *MFT1*…), recombination and DNA repair (e.g.: *EXO1*, *PES4*, *REV3*…), protein modification (e.g.: *STE14*, *APC11*, *HAT1*…), mating type determination, pheromone response and filamentous and invasive growth (e.g.: *BAR1*, *OPY2*, *GPA1*, *STE2*, *STE5*, *STE12*, *STE18*, *MFA1*, *MFA2*, *BMH2*…). These genes are induced by cAMP-activated PKA in the presence of Sch9 (compare condition 1a versus 1b in Fig. 2A) but repressed by cAMP-activated PKA in the absence of Sch9 (compare condition 2a versus 2b in Fig. 2A). Conversely, Sch9 exerts negative regulation on the expression of these genes in the absence of cAMP (compare condition1a versus 2a in Fig. 2A), but this Sch9-mediated effect is largely overruled by the presence of cAMP-activated PKA (compare condition 1b versus 2b in Fig. 2A) resulting in the overall induction of the genes (Fig. 2B). As deduced by Motif Finder, the genes of class 3 were enriched for the Ste12 binding sites known as the sterile response element (SRE) and pheromone response element (PRE). Often these sites are found in close proximity to a presumed Tec1 consensus-binding site to constitute the so-called filamentous response element (FRE) (reviewed in (Gancedo, 2001)). Ste12 has been

shown to enhance transcription of genes encoding proteins required for pseudohyphal and invasive growth (Gancedo, 2001) and of genes that are in close proximity to Ty transposable elements (Ciriacy *et al.*, 1991; Bilanchone *et al.*, 1993; Laloux *et al.*, 1994). Not surprisingly, the MIPS database annotated many of the genes in class 3 as so-called Ty-ORFs or described them to encode proteins involved in the pheromone response, mating and the pseudohyphal and invasive growth pathway. Consistent with our data and more in particular the finding that Sch9 exerts a repressive effect on *STE12*, cells deficient for Sch9 were described to display hyperactivation of the pheromone MAPK pathway and up to 5-fold higher transcription from a PRE-driven reporter construct even in the absence of pheromone (Morano and Thiele, 1999). In addition, the deletion of *SCH9* was also reported to induce hyperinvasive growth in strains of the Σ1278 background (Lorenz *et al.*, 2000) and it should be noted that this phenotype may result from the repressive effect triggered by Sch9 on different components, including not only the transcription factor Ste12 but Gcn4 as well (Braus *et al.*, 2003). Also consistent with our data are the observations that PKA plays an essential compensatory role with respect to the MAPK pathway for the induction of filamentous and haploid invasive growth ((Gancedo, 2001) and references therein). Although this compensatory role depends on different transcription factors, our data point to a more direct connection between PKA and Ste12- and/or Gcn4-dependent transcription as suggested previously (Mösch et al., 1999; Braus *et al.*, 2003).

Class 4 contains two small clusters of which only a few genes have a known function. Cyclic AMP-activated PKA represses these genes provided the presence of Sch9 (compare condition 1a versus 1b in Fig. 2A) but it induces them when Sch9 is absent (compare condition 2a versus 2b in Fig. 2A). The latter can be regarded as a compensation for the loss of Sch9 since Sch9 appears indeed to be required to maintain basal expression (Fig. 2B).

Finally, Class 5 consists of two clusters with genes encoding proteins involved in amino acid metabolism (e.g.: *LYS21*, *TRP1*, *MET10*, *LEU4*…), glycolysis, gluconeogenesis and the citric acid cycle (e.g.: *TPI1*, *ICL1*, *PCK1*, *PDC5*, *HAP4*, *IDP2*…), nitrogen metabolism (e.g.: *GAT1*, *ISU2*…) and the stress response (e.g.: *SSA2*, *SSA4*, *ZDS1*, *RSP5*…). These genes display only a minor reduction in expression when cAMP is added to the *pde2*Δ *cyr1*Δ *msn2*Δ *msn4*Δ strain and hence they do not respond significantly to cAMP if Sch9 is present (compare condition 1a versus 1b in Fig. 2A). In contrast, these genes show a marked drop in expression when *SCH9* is deleted, indicating that they are primarily regulated by the Sch9 kinase (compare condition 1a versus 2a in Fig. 2A). Interestingly, however, cAMP-activated PKA could restore expression to some extent in the absence of Sch9 (compare condition 2a versus 2b in Fig. 2A), which is indicative for the compensation for the loss of Sch9 function (Fig. 2B).

Taken together, based on the expression profiles (Fig. 2A) it appears that Sch9 is required to maintain basal expression levels for most genes in the absence of cAMP-activated PKA. Indeed, upon deletion of *SCH9*, the expression dropped to a minimum level for the 392 genes found in classes 1, 4 and 5 while it increased to maximal levels for the 236 genes of class 3. For most of these genes, expression is restored, at least in part, when cAMP is supplemented. Also for the 290 genes of class 2, expression decreased in the *sch9*Δ mutant but in many of these cases, the lack of Sch9 compromised further repression by cAMP-activated PKA. Most interestingly, the effects exerted on expression by the combined action of both Sch9 and cAMP-activated PKA were reversed for one (*i.e*. Sch9 in class 2) or both kinases (classes 3-5) if they were acting alone. These opposed effects are summarised in Figure 2B and they led us to conclude that PKA and Sch9 most likely control a molecular switch that triggers opposed transcriptional effects of the genes in each of these classes.

Sch9 positively controls PDS-driven gene expression through Gis1, independently of Rim15.

As mentioned above, we found the so-called STRE-element to be enriched in class 2 genes. This STRE-element is known to be bound by the PKA-controlled Msn2 and Msn4 transcription factors in response to a variety of stresses (Martinez-Pastor *et al.*, 1996). However, it was rather unexpected that so many of the STRE-controlled genes were still found in our genome-wide expression analysis since the strains used in this study carried deletions for both transcription factors. This strongly indicated that other factors contribute to the regulation of the STRE-controlled genes. For some of these genes, additional regulation may involve the transcriptional activator Gis1 since its corresponding DNA binding element, known as PDS (post diauxic shift) (Boorstein and Craig, 1990; Pedruzzi *et al.*, 2000) was also overrepresented in the same class (Table 2, and supplementary data in Table S2). The PDS element confers derepression during the diauxic shift when glucose becomes limiting and thus provides expression regulation similar to that conducted by the STRE-element (Pedruzzi *et al.*, 2000). Its core closely resembles the STRE-consensus sequence and therefore it is plausible that Gis1 and Msn2/4 may have partially overlapping functions dependent on the promoter context and thus that Gis1 may account for the regulation on the STRE-sites in the absence of Msn2/4. Such a functional redundancy is further supported by the observation that both Gis1 and Msn2/4 are not only positively controlled (Pedruzzi *et al.*, 2000) but also mediate almost the entire transcriptional response regulated by the protein kinase Rim15, with a significant overlap between the targets affected by each of the transcription factors (Cameroni *et al.*, 2004). Rim15 is immediately downstream and negatively controlled by PKA (Reinders *et al.*, 1998) and it defines the convergence of PKA, Sch9 and TOR signalling (Pedruzzi *et al.*, 2003). Interestingly, the latter

study reported that although being a negative regulator of Rim15 nuclear accumulation, Sch9 also acts independently of Rim15 as an activator of the Rim15-controlled transcriptional responses. Based on the genome-wide expression data and as mentioned above, REDUCE calculated that Sch9 does not correlate with the STRE-motif while it shows a positive correlation with the PDS motif as opposed to the negative correlations calculated for PKA (Table 2, Table 3). Therefore, it would be more than likely that the Rim15-independent role of Sch9 for transcription activation would be mediated through Gis1. To test this possibility, we monitored expression of prototype Gis1-dependent PDS-driven genes (*GRE1*, *SSA3*) and Msn2/4-dependent STRE-driven genes (*DDR2*, *HSP12*). These genes are all repressed in wild type cells exponentially growing on glucose-containing medium and become induced or derepressed when the cells are shifted to glycerol-containing medium, a condition that mimics the diauxic shift (Fig. 4A). In agreement with the data previously reported, derepression of the PDS-controlled *SSA3* gene was comparable to wild-type cells in the *msn2Δ msn4Δ* strain (Martinez-Pastor *et al.*, 1996), significantly reduced in the single *rim15Δ* strain and completely absent in strains bearing a deletion of *GIS1* (Pedruzzi *et al.*, 2000). Similar effects were observed for the PDS-controlled *GRE1* gene (Garay-Arroyo and Covarrubias, 1999) although expression levels were lower in the *msn2Δ msn4Δ* strain than in the wild type strain indicating that Msn2/4 might also regulate PDS-driven transcription. As predicted based on the REDUCE calculations, the strains with a deletion of *SCH9* completely failed to derepress *SSA3* and *GRE1* after the carbon source shift, indicating that Sch9 is essential to maintain Gis1-mediated transcription of the PDS-driven genes. Noteworthy, this effect was stronger than that triggered by the lack of Rim15 which confirms that the requirement of Sch9 for derepression of the PDS-driven genes cannot solely be explained based on its reported control of the nucleocytoplasmic distribution of Rim15 but that additional Rim15-independent mechanisms

Fig. 4

have to be involved. Also in line with the REDUCE calculations is that, neither Gis1 nor Sch9 appeared to be essential for the derepression of the STRE-driven genes *HSP12* and *DDR2* since there was no significant effect in the single *gis1*Δ or *sch9*Δ mutants as compared to the wild-type strain. Nonetheless, the residual expression of *HSP12* and *DDR2* observed in the *msn2Δ msn4Δ* strain was completely absent in the *msn2Δ msn4Δ gis1Δ* strain suggesting that Gis1, Msn2 and Msn4 cooperatively regulate STRE/PDS driven gene expression. This cooperative effect of Gis1 was further confirmed by comparison of the expression levels of *HSP12* and *DDR2* between the *sch9Δ rim15Δ msn2/4Δ* and the *sch9Δ gis1Δ msn2/4Δ* quadruple mutants where the expression was again completely annihilated in the latter strain (Fig. 4A). Also for Sch9, its role in the expression regulation of the STRE-driven genes becomes more apparent when multiple deletion strains are taken into account but, consistent with the data obtained from the genome-wide expression analysis, this role seems to be dual. Indeed, the expression levels of *HSP12* and *DDR2* were significantly lower in the *sch9*Δ *gis1*Δ mutant when compared to the single *gis1*Δ mutant, indicating that Sch9 may exert a positive function, whereas these expression levels were dramatically induced in the *sch9Δ rim15Δ* mutant when compared to the single *rim15*Δ mutant, which would be consistent with Sch9 acting as negative regulator. Note that the strongly increased expression of *HSP12* and *DDR2* in the *sch9Δ rim15Δ* strain is predominantly accounted for by Msn2 and Msn4 since only a low expression was observed in the *sch9Δ rim15Δ msn2/4Δ* strain (Fig. 4A). Thus, while our data indicate that Sch9 controls the expression of the PDS-driven genes independently of Rim15, they suggest that Sch9 may function as a positive or negative regulator for the expression of STRE-driven genes dependent on the presence or absence of Rim15.

To elaborate on the roles of Rim15 and Sch9 on STRE/PDS-driven expression, we examined whether these kinase would influence the cellular distribution of Gis1 or Msn2/4. Therefore, strains were transformed with GFP-tagged versions of these transcription factors and the transformants were tested under conditions known to influence nuclear accumulation of Msn2/4, i.e. glucose-exhaustion and rapamycin-addition to glucose-grown cells (Fig. 4B). The data showed that neither the deletion of *SCH9* nor that of *RIM15* has any effect on the nucleocytoplasmic translocalization of Msn2/4. For Gis1, our results showed that this transcription factor is always nuclear localized independent of whether or not Sch9 or Rim15 are present (Fig 4B). Therefore, the requirements of Sch9 or Rim15 to regulate Gis1- and Msn2/4-mediated transcription should either be direct through changes in phosphorylation of these factors or indirect via alterations in global transcription complexes. Concerning the latter, our genome-wide expression analysis identified *CAF4, NOT5*, *ADA2*, *SPT7* and *TRA1* as targets of Sch9 and cAMP-activated PKA.

Taken together, our Northern blot analyses provide an explanation for our initial observation that PKA and Sch9 oppositely control PDS-driven gene expression (class 2 in Fig. 2A; Table 3) as they point to an independent positive regulatory effect of Sch9 and Rim15 to sustain proper Gis1 activity. They also corroborate the apparent PKA-dependent conversion of the function of Sch9 from a positive to a negative regulator as concluded from the genome-wide expression analysis (class 2 in Fig. 2A) and demonstrate the importance of Rim15 for this phenomenon. Consequently, this conversion may explain the lack of a strict correlation between Sch9 and the control of STRE-driven genes as calculated by REDUCE (Table 2). Finally, the Northern blot analyses substantiated the redundancy between Gis1 and Msn2/4, which is further supported by the fact that the triple *msn2*Δ *msn4*Δ *gis1*Δ mutant as well as the quadruple mutants *sch9*Δ *msn2*Δ *msn4*Δ *rim15*Δ and *sch9*Δ *msn2*Δ *msn4*Δ *gis1*Δ displayed a pronounced synthetic

474 growth defect on rich glycerol-containing medium while the double mutants *msn2*Δ *msn4*Δ,
475 *sch9*Δ *rim15*Δ and *sch9*Δ *gis1*Δ displayed no or only a partial growth phenotype (Fig. 4C).

Discussion

In this study, the relationship between the AGC protein kinases PKA and Sch9 in *S. cerevisiae* was investigated. Although it was previously suggested that Sch9 might act as an upstream cAMP-independent nutritional regulator of PKA (Crauwels *et al.*, 1997), our data indicate that both kinases control separate but partially redundant signal transduction pathways: (i) Sch9 controls growth regulatory functions independently of PKA and its downstream effectors Msn2/4, (ii) cAMP-activated PKA and Sch9 are separate and distinguishable requirements for glucose-induced trehalase activation, (iii) PKA and Sch9 appear to have a limited number of specific targets genes and both kinases trigger synergistic as well as opposed effects on the expression of a larger group of common target genes.

Figure 5

Sch9 and Rim15 control a molecular switch.

When we first described the involvement of Sch9 in nutrient signalling we demonstrated that cells lacking Sch9 showed phenotypic characteristics during growth on a non-fermentable carbon source that are usually associated with higher PKA activity while they could not maintain these high PKA phenotypes during fermentative growth (Crauwels *et al.*, 1997). Given that growth of wild-type cells on a non-fermentable carbon source is usually described as to correspond with low PKA activity and fermentative growth of wild-type cells with high PKA activity, one may conclude that deletion of *SCH9* triggers a switch that seems to reverse the correlation between PKA and the available carbon source. This switch is consistently reflected in our microarray data where indeed the combined action of both Sch9 and PKA (comparison 1a versus 1b in Fig. 2A) often triggers opposite transcriptional responses when compared to the responses triggered by either PKA (comparison 2a versus 2b in Fig. 2A) or Sch9 (comparison 1a

versus 2a in Fig. 2A). More recently, we showed that PKA- and Sch9-dependent signalling converges on the protein kinase Rim15 and we demonstrated that the role of Sch9 was to prevent nuclear accumulation of Rim15 as to keep the kinase in the cytoplasm where it can be inactivated by PKA-phosphorylation. We then also noticed that besides its role as a negative regulator of Rim15 nuclear import, Sch9 exerted additional control on Rim15-responses independently of Rim15 (Pedruzzi *et al.*, 2003). The data presented in this paper confirm this and point to the involvement of the Rim15-effector Gis1 as we found Sch9 to be absolutely required for Gis1-dependent transcription of PDS-driven genes. On the other hand, Sch9 appeared not to be essential for derepression of STRE-driven genes, which is largely accounted for by Msn2/4. Nonetheless, as mentioned above, comparison of the single *gis1*Δ deletion strain with the *sch9*Δ *gis1*Δ indicated a positive control of Sch9 on STRE-transcription while the comparison of the single *rim15*Δ with the *sch9*Δ *rim15*Δ strain suggested a negative control of Sch9 on the same genes. Thus, dependent on the presence or absence of Rim15, Sch9 appears to switch from a positive to a negative regulator of STRE-driven gene expression. This altered effect of Sch9 on STRE-driven expression, however, may involve both Msn2/4 and Gis1 and it can be direct or indirect but so far we can only guess about the underlying mechanisms. One explanation would be that Sch9 and/or Rim15 regulate the interaction between Msn2/4 or Gis1 with global transcription complexes as to sustain proper STRE- and PDS-driven transcription. This may, indeed, not only require changes of Msn2/4 or Gis1 but additionally or alternatively also adaptations in the global transcription complexes as to make them compatible for interaction with Msn2/4 or Gis1. Although we did not study the mode-of-action of Sch9 and Rim15 in detail, several observations support the involvement of the latter mechanism. First, Sch9 and Rim15 do not alter the subcellular localization of Msn2 or Gis1. Second, we identified several genes encoding subunits of diverse global transcription complexes to be targets of Sch9 and cAMP-

activated PKA. Third, a mode of action on general transcription complexes would be in line with previously reported data showing that a subunit of Ccr4-Not, i.e. Not5, a subunit shared between TFIID and SAGA, i.e. Taf25, as well as components of the histone deacetylase (HDAC) complex, i.e. Sin3 and Rpd3, have all been described as possible effectors of Rim15 (Kirchner *et al.*, 2001; Lenssen *et al.*, 2002; Pnueli *et al.*, 2004). Thus, the combined action of Rim15 and Sch9 on the regulation of PDS/STRE-driven gene expression might be far more complicated than the simple activation or inactivation of Msn2/4 and Gis1.

Gis1 and Msn2/4 have partially redundant functions.

Compelling evidence suggests that the Gis1 and Msn2/4 transcriptional activators cooperatively regulate STRE/PDS-driven gene expression. We noticed before that Msn2/4 and Gis1 largely control the Rim15 regulon upon nutrient limitation (Cameroni *et al.*, 2004). In this study we observed a significant cAMP-mediated decrease of STRE-driven genes in strains devoid of *MSN2/4* (Class 2 genes). Most of these genes harboured additional or partially overlapping PDS elements in their promoter and for two of those, i.e. *HSP12* and *DDR2*, we could demonstrate that Gis1 indeed mediated their transcription (Table 2 and Table 3). Given the similarities between the STRE and PDS consensus sites, one may consider to extend the transcriptional regulation by Gis1 to genes containing only perfect STRE elements. This would not be without precedent since Gis1 has been reported to modulate the expression of *PHR1* gene and a derived reporter construct containing the STRE-consensus sequence (Jang *et al.*, 1999). Conversely, Msn2/4 may as well be able to regulate PDS-driven gene expression as we observed for the *GRE1* gene, a gene that contains only PDS-consensus sequences in its promoter. However, it cannot be excluded that in both cases of cross-regulation, i.e. STRE-driven genes by Gis1 and PDS-driven genes by Msn2/4, other transcription factors and yet unidentified DNA

548 elements may be involved. Nevertheless, the redundant function of Msn2/4 and Gis1 is further
549 exemplified by the observation that the *msn2/4*Δ *gis1*Δ strain displays a synthetic lethal
550 phenotype on glycerol-containing medium while the *msn2/4*Δ and *gis1*Δ mutants do not show an
551 apparent growth defect under these conditions.
552
553 *PKA, Sch9 and the Tor kinases as constituents of a nutritional integrator mechanism.*
554 We previously reported that rapamycin-induced inhibition of the Tor kinases and deletion
555 of *SCH9* both triggered nuclear accumulation of Rim15 (Pedruzzi *et al.*, 2003). In this paper, we
556 show that the deletion of *SCH9* or *RIM15* does not affect the nucleocytoplasmic distribution of
557 Gis1 or the nuclear translocation of Msn2 upon glucose starvation or rapamycin supplementation.
558 Especially the latter is interesting because it further discriminates between the mode-of-action of
559 the Sch9 and TOR kinases, which have both been implicated in sensing of glucose and other
560 nutrients, especially the availability of nitrogen. Indeed, in contrast to Sch9, the Tor kinases are
561 known to promote nuclear export of Msn2 (Beck and Hall, 1999; Mayordomo *et al.*, 2002).
562 Hence, this observation not only confirms that Sch9 is operating in a parallel pathway with
563 respect to the Tor kinases, but it further supports the idea that Sch9 controls changes in
564 transcription of the stress-responsive genes mainly via Gis1 and Rim15 while TOR may control
565 the expression of stress-responsive genes mainly via Msn2/4 and Rim15. This would further be
566 consistent with data obtained on longevity showing that the increased life span of an *sch9*Δ strain
567 can be partially suppressed by the additional deletion of *RIM15* but not by the additional deletion
568 of *MSN2* and *MSN4* whereas the increased lifespan of a *cyr1*Δ mutant can be suppressed by both
569 deletion of *RIM15* or *MSN2/4* (Fabrizio *et al.*, 2001). It is also in agreement with our initial
570 observation that the combined deletion of *MSN2* and *MSN4* suppresses only the requirement of
571 PKA, but not the requirement of Sch9 for growth (Fig. 1A). Here it should also be noted that the

additional deletion of *MSN2* and *MSN4* and activation of PKA by supplementation of extracellular cAMP do only support fermentative growth of the *pde2Δ cyr1Δ* mutant while it requires overexpression of *SCH9* to obtain growth under both fermentative as well as non-fermentative conditions. This Sch9-dependent phenotype appears to be independent of the activity of PKA or the presence of Msn2/4. Since in the absence of Msn2/4, Gis1 becomes essential for growth on non-fermentable carbon sources, perhaps it requires overexpression of Sch9 to obtain enough Gis1 to force transcription of otherwise Msn2/4-controlled genes. Expression profiles from our micro-array analysis that would fit best this description are those found in class 2, cluster 5 and 6. These clusters contain indeed STRE-driven genes that show dramatically reduced expression in the *pde2Δ cyr1Δ msn2Δ msn4Δ* mutant under conditions of cAMP-activated PKA as well as deletion of *SCH9* but highly enhanced expression upon overexpression of Sch9. Based on their functional classification, these genes encode proteins with roles in a variety of processes or with yet unknown functions (see http://www.kuleuven.ac.be/bio/mcb/allratio). Of particular interest are *UBC1*, *MSW1* and *SDS22* of which the null mutants display pronounced growth defects.

Given the partial redundancy between Gis1 and Msn2/4 (this study and (Cameroni *et al.*, 2004)), and their differential regulation the Sch9 pathway and the TOR pathway, one may look at the Sch9 pathway and the TOR pathway as counterbalancing systems that are part of a nutritional integrator allowing to fine tune transcription of stress-responsive genes. This led us to the model presented in Fig. 5. In this model, a central position is hold by PKA, which inactivates the cytoplasmic localized Rim15, i.e. the common target of Sch9 and TOR signaling (Pedruzzi *et al.*, 2000; Pedruzzi *et al.*, 2003). Since the activity of PKA is dramatically increased at the beginning of fermentation via a glucose-induced boost of cAMP (Thevelein *et al.*, 2000) and decreased at

595 the end of fermentation because of enhanced expression of its regulatory subunit, Bcy1 (Werner-
596 Washburne *et al.*, 1993), it is feasible to assume that the PKA-Rim15 module is providing
597 contextual information regarding the presence of a fermentable carbon source. As such, this
598 system resembles a phenomenon recognized in higher eukaryotes and described as cAMP-gating
599 (Iyengar, 1996; Jordan and Iyengar, 1998) where a main gatekeeper, the protein kinase PKA,
600 enhances, blocks or redirects signal flow through primary signal transduction cascades. In yeast,
601 the phenomenon of cAMP-gating is supported by the data described in this paper showing that
602 transcriptional responses mediated by Sch9 are in many cases counteracted or reversed when
603 PKA became activated by cAMP. Also for TOR there is evidence for cAMP gating since
604 constitutive activation of the RAS-cAMP signaling pathway confers resistance to rapamycin and
605 prevents, similar to deletion of *RIM15*, several rapamycin-induced responses (Pedruzzi *et al.*,
606 2003; Schmelzle *et al.*, 2004).

607 Similar principles of nutritional integration may as well apply to the formation of
608 pseudohyphae and the invasive growth in reaction to nutrient limitation, most notably nitrogen
609 limitation. Pseudohyphal and invasive growth is believed to facilitate foraging for nutrients under
610 adverse conditions. The control of this transition involves several signal transduction pathways,
611 including the Ras-cAMP pathway and a MAPK pathway that shares components of the
612 pheromone pathway. Consistent with their reported roles in nitrogen sensing, also the TOR- and
613 Sch9-pathway appear to be involved in the control of this morphological switch (Lorenz *et al.*,
614 2000; Cutler *et al.*, 2001). TOR plays a positive role since its inhibition following rapamycin
615 treatment was found to prevent pseudohyphal and invasive growth of diploid cells. The role of
616 Sch9, on the other hand, is more ambiguous as it was reported only to be a minor player in the
617 transition of diploids while it acts as an inhibitor of invasive growth of haploid cells. The latter is
618 consistently reflected in our genome-wide expression analysis where Sch9 was found to repress

619 the expression of several key components required to make the transition to invasive growth (see
620 genes of Class 3). Although the function of the Sch9 kinase in haploids appears thus to be the
621 opposite of that of the Tor kinases in diploids, in both cases were the changes associated with the
622 inhibition or deletion of these kinases corrected by increased PKA activity (this study; (Gancedo,
623 2001; Cutler *et al.*, 2001)). It should be mentioned that our micro-array results clearly
624 demonstrated that deletion of *SCH9* results in a dramatic increase of several *STE* genes under
625 conditions of low PKA activity, a phenomenon that is compensated by cAMP-activation of PKA.
626 For *STE12*, for instance, it has been shown that cells cannot tolerate high levels of expression
627 (Dolan and Fields, 1990). Therefore, the observed dramatic enhanced transcription and
628 deregulation of other pheromone pathway components upon deletion of *SCH9* in the *pde2Δ*
629 *cyr1Δ msn2Δ msn4Δ* mutant may provide another explanation why the lack of Sch9 in
630 combination with low PKA may cause growth arrest.
631
632 *Conclusion*
633 To summarise, this paper provides further evidence that PKA and Sch9 function in
634 parallel signalling pathways that converge on the protein kinase Rim15 and its downstream
635 effectors Msn2/4 and Gis1. In addition to the previously reported role of Sch9 as negative
636 regulator of nuclear import of Rim15, our data demonstrate that Sch9 positively regulates Gis1-
637 dependent PDS-driven gene expression independently of Rim15. Furthermore, the data presented
638 confirm the notion that Msn2/4 and Gis1 cooperatively regulate STRE/PDS-driven gene
639 expression. The knowledge that TOR-signalling controls nuclear export of Rim15 as well as of
640 Msn2/4, led us to postulate the existence of a nutritional integrator system to fine-tune the
641 expression of stress-responsive genes. This system is controlled by the two counterbalancing

642 pathways, the Sch9 pathway on one hand, and the TOR pathway on the other, and with PKA and
643 Rim15 as central core. Also other phenotypic read-outs appear to be regulated by the concerted
644 action of Sch9, PKA and the Tor kinases and thus they may be regulated by a similar principle of
645 nutritional integration.

Experimental Procedures

Table 4

Strains, plasmids and growth media

Yeast strains are listed in Table 4 (Thomas and Rothstein, 1989; Martinez-Pastor *et al.*, 1996; Smith *et al.*, 1998). Deletions were made using either plasmid derived or polymerase chain reaction-derived disruption cassettes as described previously (Brachmann *et al.*, 1998). The plasmid YIp*SCH9* expresses *SCH9* under control of the strong *TPI* promoter while YCplac111/*SCH9* expresses *SCH9* from its own promoter. Plasmids YCp*ADH1-GIS1* (Pedruzzi *et al.*, 2000), YCpADH1-*RIM15* (Reinders *et al.*, 1998) and pADH1-*MSN2GFP* (Gorner *et al.*, 1998) were previously described. Plasmids expressing *BCY1* (181pBGHB) and *TPK1* (33pAGT) have been described (Griffioen *et al.*, 2000). GPF-tagged version of Gis1 was expressed under the control of the *ADH1* promoter in a low copy number plasmid pNP305. For β-galactosidase assays, plasmid pJS205XXB (kindly provided by J. Schüller; (Myers *et al.*, 1986)) containing a truncated minimal *CYC1* promoter in front of LacZ was used. Primers N1a (TCGAGGCTAGCTGAAAAAA), N1b(GATCTTTTTTCAGCTAGCC), N3a (TCGAGGCTAGCTAAGGA), N3b (GATCTCCTTAGCTAGCC), N4a (TCGAGGCTAGCAAACGA) and N4b (GATCTCGTTTGCTAGCC) were heated and annealed by slow cooling to generate the double stranded (ds) oligos N1, N3 and N4 that contain the DNA-motifs corresponding to RRPE, U4 and PDS (underlined), respectively, flanked by XhoI and BamHI overhangs and a unique NheI restriction site. After 5'-phosphorylation, these ds-oligos (T4 polynucleotide kinase) were ligated (T4 DNA ligase) into the XhoI/BamHI-cut vector pJS205XXB generating plasmids pJS205XN1B, pJS205XN3B and pJS205XN4B respectively. Constructs were checked by NheI restriction and DNA sequencing for proper oligo-incorporation. Yeast cells were grown at 30°C in rich medium YP (yeast extract-peptone) supplemented with

either 2% galactose (YPGal), 2% glycerol / 2% ethanol (YPGE) or 2% glucose (YPD, ScD) as described (Sherman *et al.*, 1986). Cyclic AMP was added in excess at a concentration of 3 mM on agar plates or at a concentration of 0.5 mM in liquid medium. Transformation of strains was done as described previously (Gietz *et al.*, 1995).

Viability tests, growth assay

To test the viability after cAMP starvation, cells of the strains *pde2*Δ *cyr1*Δ *msn2/4*Δ (GG104) and *pde2*Δ *cyr1*Δ *msn2/4*Δ *sch9*Δ (RJ_100A) were starved for cAMP for 0, 6 and 24 hours. Dilution series (starting $O.D._{600}$ at 0.2) were spotted on YPD plates with or without cAMP and incubated at 30 °C for 2 days and the numbers of colonies were compared. For the other growth assays, strains were grown overnight in 5 ml preculture YPD, $O.D._{600}$ was measured and 10 µl of a 10 fold 1/10000 dilution series with starting $O.D._{600}$ of 0.2 was plated out and incubated for 2 days at 30°C.

Genome-wide gene expression analysis

Experiment and sample taking were done twice for two independent colonies. Strains were grown to mid-exponential phase (OD 0.5) in 100 ml YPGal with 0.5 mM cAMP. Subsequently, the cells were washed twice with YPGal, resuspended and allowed to grow further in 100 ml YPGal. After 6 hours, the culture was divided into two equal fractions (2x 50 ml) and 3 mM cAMP was added to one fraction. Both fractions were then grown for another hour. RNA was extracted using RNApure™ (GeneHunter® Corporation, Nashville, USA, cat n° P501) according the protocol supplied by the company and diluted to a final concentration of 1 µg/µl for cDNA preparation and labelling (1 µg RNA; α^{33}PdCTP) using Superscript II (Invitrogen, cat n° 18064-014). Serial

693 hybridization on Yeast Index GeneFilters (Research Genetics/Invitrogen, Huntsville, GF100) was
694 performed according delivered protocol (Research Genetics/Invitrogen). Images were scanned
695 (FUJIX Bas1000) and analyzed using the program Pathways 3.0 (Research Genetics). Duplicate
696 experiments were performed on new filter sets. Selected genes were manually flagged for
697 hybridization artefacts. Gene annotations were derived from the MIPS (Munich Information
698 Centre for Protein Sequences) functional categories. Analysis of the control spots, present on the
699 Yeast Gene Filters® Microarrays, showed a pronounced multiplicative error in the data (i.e. the
700 absolute error on measurements increases with the measured intensity). Therefore, raw intensity
701 measurements were log-transformed. To allow for across-filter comparisons of expression values,
702 these log-transformed measurements were mean-centered per filter. Statistical analysis of the
703 resulting data for the control spots led us to assume the error on the log-transformed data was
704 normally distributed with variance 0.10006 and mean 0. The fold changes of 1.5, 2 and 3, as used
705 throughout the article for selecting genes with differential expression between two conditions,
706 thus correspond to confidence levels of 0.90, 0.99 and 0.9995 respectively. Data are freely
707 available at http://www.kuleuven.ac.be/bio/mcb/allratio following the MIAME recommendation.
708 Enrichment factors for each functional category were calculated as described previously
709 (Tavazoie *et al.*, 1999). Genes with the highest variance across their expression profile
710 (approximately one third of all genes) were clustered using the Adaptive Quality Based
711 Clustering algorithm (AQBC; significance parameter was set to 0.80) as described by De Smet *et*
712 *al*., 2002. This resulted in 918 genes being assigned to 14 different clusters.
713 The program REDUCE (Bussemaker *et al.*, 2001) was used to discover oligonucleotide motifs
714 whose occurrence in the promoter region of a gene correlates with changes in its expression level.
715 All oligonucleotides up to length 7 were tested and matches were counted in a window of 600 nt
716 upstream of each ORF (a truncated window was used whenever necessary to avoid overlap with

upstream ORFs on either strand). Putative motifs were screened against the TRANSFAC database (Heinemeyer *et al.*, 1998). Using a P-value cut-off of 0.01, their PKA and/or Sch9 dependency was evaluated for each of the pair-wise comparisons based on the F-scores for each element. The most significant motifs (Table 2) were tested for their abundance in each gene cluster (Fig. 3A) using Regulatory Sequence Analysis Tools (van Helden *et al.*, 2000). Distribution of these elements for each class relative to their genome-wide distribution was calculated according the algorithm described previously (Tavazoie *et al.*, 1999). Motifs were deemed to be statistically overrepresented when the minus log2(p-value) exceeded 1.

To detect statistically overrepresented motifs in the sets of co-expressed genes (clusters), we used Motif Sampler, a motif detection algorithm based on Gibbs sampling (Thijs *et al.*, 2002). Yeast intergenic sequences were retrieved from RSA tools (van Helden *et al.*, 2000). By using multiple runs of the algorithm and testing different parameter settings, motifs with a high consensus score, a high number of occurrences in the set of co-expressed genes and that were retrieved consistently were retained. These putative motifs were screened against the TRANSFAC database (Heinemeyer *et al.*, 1998) and only motifs for which a description was available in Transfac were further investigated.

Northern blot analysis

For microarray confirmation, strains were grown in the same way. Hybridization was done using cDNA probes of randomly chosen genes of different clusters. For diauxic shift experiment, strains were grown on YPD medium. At mid-exponential phase ($O.D._{600}$ = 0.5), samples were taken at 30' and 15' before the cells were collected and washed in YPGE medium and resuspended in YPGE. Then, samples were taken after 15', 30' and 60' incubation in YPGE

medium. RNA extraction and hybridization was performed using the protocol described previously (Crauwels *et al.*, 1997). Hybridized filters were exposed to phosphorimager screens and images were scanned with FUJIX Bas1000. Quantification of northern blot images was done with Tina 2.0.

Trehalase Enzyme Assays

Strains GG104, RJ_100A and RJ_102 were grown to exponential phase on YPGal in the presence of 0.5 mM cAMP. Cells were collected by centrifugation, washed twice with YPGal and resuspended in fresh YPGal supplemented with or without 0.5 mM cAMP. Other strains were grown on YPGal. 100mM glucose was added after a 20 minutes pre-incubation period at 30°C. Trehalase activity (nmol glucose min^{-1} mg $protein^{-1}$) in crude cell extracts was determined as described previously (Mitsuzawa, 1993). Average values over at least 3 independent measurements are shown with an average standard deviation of 2.19.

Galactosidase Assays

Exponential growing cells were collected by centrifugation and resuspended in ice cold breaking buffer containing 1/10 solution of dissolved proteinase inhibitor cocktail tablets (Complete Mini, EDTA free, Roche Diagnostics). Cells were broken using glass beads. Ten µl of clarified protein extract was diluted to a total volume of 0.5 ml breaking buffer and incubated at 30°C for 5' and the reaction was initiated by adding 0.1 ml of 4mg/ml ONPG (o-Nitrophenylgalactoside). At precise time the reaction was terminated by addition of 0.25 ml 1M Na_2CO_3. $O.D._{420}$ was measured (BioPhotometer, Eppendorf) and protein concentration was determined according the Bradford method. Specific activity was calculated by the formula ($O.D._{420}$*1.7)/(0,0045*protein conc.*extract volume*time). The specific background activity (empty vector) was subtracted

764 from the specific activity of the sample (reporter vector) giving the samples actual specific
765 activity (nmoles min^{-1} mg $protein^{-1}$). Experiments were done in triplicate for independent
766 colonies. Error estimation was calculated as the square root of ((sum of squares of standard
767 deviations)/number of measurements).
768
769 *Green fluorescence protein (GFP) fluorescence microscopy.*
770 Cells expressing GFP-tagged Msn2 or Gis1 were used directly without fixation. Nuclei were
771 stained by addition of 1 μg of DAPI (4',6'-diamidino-2-phenylindole) per ml cell culture. Cells
772 were viewed using a Zeiss Axioplan 2 fluorescence microscope. Images were taken with an
773 AxioCam HRm charge-coupled device camera using AxionVision 3.0 software.

Acknowledgements

We are thankful to A. Tanghe for thorough introduction into microarray technology, to J. Rosseels for excellent technical assistance and to N. Vangoethem for website support. We are grateful for fellowships from the Institute for the Promotion of Innovation through Science and Technology (IWT-Vlaanderen) to J.R. and K.E., the Fund for Scientific Research-Flanders (FWO) to K.M. and G.G. and the Research Fund of the Katholieke Universiteit Leuven to J.M. This work was supported by grants from the Roche Foundation to L. C., The Swiss National Science Foundation (631-062731) to C.D.V., the Fund for Scientific Research-Flanders to J.W. and B.D.M., the Research Fund of the Katholieke Universiteit Leuven (OT-TBA, GOA: Concerted Research Actions and IDO: Interdisciplinary Research Action) to J.W., J.M.T. and to B.D.M., the Federal Service for Scientific, Technological and Cultural Affairs (DWTC-IUAP-program) to J.M.T. and to B.D.M. and the Institute for Scientific and Technological Research to B.D.M.

References

Beck, T., and Hall, M.N. (1999). The TOR signalling pathway controls nuclear localization of nutrient-regulated transcription factors. Nature *402*, 689-692.

Belazzi, T., Wagner, A., Wieser, R., Schanz, M., Adam, G., Hartig, A., and Ruis, H. (1991). Negative regulation of transcription of the Saccharomyces cerevisiae catalase T (CTT1) gene by cAMP is mediated by a positive control element. Embo J *10*, 585-592.

Bilanchone, V.W., Claypool, J.A., Kinsey, P.T., and Sandmeyer, S.B. (1993). Positive and negative regulatory elements control expression of the yeast retrotransposon Ty3. Genetics *134*, 685-700.

Boorstein, W.R., and Craig, E.A. (1990). Transcriptional regulation of Ssa3, an Hsp70 gene from *Saccharomyces cerevisiae*. Mol. Cell. Biol. *10*, 3262-3267.

Boy-Marcotte, E., Perrot, M., Bussereau, F., Boucherie, H., and Jacquet, M. (1998). Msn2p and Msn4p control a large number of genes induced at the diauxic transition which are repressed by cyclic AMP in *Saccharomyces cerevisiae*. J. Bacteriol. *180*, 1044-1052.

Brachmann, C.B., Davies, A., Cost, G.J., Caputo, E., Li, J.C., Hieter, P., and Boeke, J.D. (1998). Designer deletion strains derived from *Saccharomyces cerevisiae* S288C: a useful set of strains and plasmids for PCR-mediated gene disruption and other applications. Yeast *14*, 115-132.

Braus, G.H., Grundmann O., Brückner, S., and Mösch H.-U. (2003) Amino acid starvation and Gcn4p regulate adhesive growth and Flo11 gene expression in Saccharomyces cerevisiae. Mol. Biol. Cell *14*, 4272-4284

Bussemaker, H.J., Li, H., and Siggia, E.D. (2001). Regulatory element detection using correlation with expression. Nat Genet *27*, 167-171.

Cameroni, E., Hulo, N., Roosen, J., Winderickx, J., and De Virgilio, C. (2004). The Novel Yeast PAS Kinase Rim15 Orchestrates G(0)-Associated Antioxidant Defense Mechanisms. Cell Cycle *3*.

Ciriacy, M., Freidel, K., and Lohning, C. (1991). Characterization of trans-acting mutations affecting Ty and Ty-mediated transcription in Saccharomyces cerevisiae. Curr Genet *20*, 441-448.

Crauwels, M., Donaton, M.C., Pernambuco, M.B., Winderickx, J., de Winde, J.H., and Thevelein, J.M. (1997). The Sch9 protein kinase in the yeast Saccharomyces cerevisiae controls cAPK activity and is required for nitrogen activation of the fermentable-growth-medium-induced (FGM) pathway. Microbiol. *143*, 2627-2637.

Cutler, N.S., Pan, X., Heitman, J., and Cardenas, M.E. (2001). The TOR signal transduction cascade controls cellular differentiation in response to nutrients. Mol Biol Cell *12*, 4103-4113.

De Smet, F., Mathys, J., Marchal, K., Thijs, G., De Moor, B., and Moreau, Y. (2002). Adaptive quality-based clustering of gene expression profiles. Bioinformatics *18*, 735-746.

Dequard-Chablat, M., Riva, M., Carles, C., and Sentenac, A. (1991). RPC19, the gene for a subunit common to yeast RNA polymerases A (I) and C (III). J. Biol. Chem. *266*, 15300-15307.

Dolan, J.W., Fields, S. (1990). Overproduction of the yeast STE12 protein leads to constitutive transcriptional induction. Genes Dev *4*, 492-502.

Doskeland, S.O., Maronde, E., and Gjertsen, B.T. (1993). The genetic subtypes of cAMP-dependent protein kinase--functionally different or redundant? Biochim Biophys Acta *1178*, 249-258.

Fabrizio, P., Liou, L.L., Moy, V.N., Diaspro, A., SelverstoneValentine, J., Gralla, E.B., and Longo, V.D. (2003). SOD2 Functions Downstream of Sch9 to Extend Longevity in Yeast. Genetics *163*, 35-46.

834 Fabrizio, P., Pozza, F., Pletcher, S.D., Gendron, C.M., and Longo, V.D. (2001). Regulation of
835 longevity and stress resistance by Sch9 in yeast. Science *292*, 288-290.
836 Francois, J., Van Schaftingen, E., and Hers, H.G. (1984). The mechanism by which glucose
837 increases fructose 2,6-bisphosphate concentration in Saccharomyces cerevisiae. A cyclic-AMP-
838 dependent activation of phosphofructokinase 2. Eur. J. Biochem. *145*, 187-193.
839 Gancedo, J.M. (2001). Control of pseudohyphae formation in Saccharomyces cerevisiae. FEMS
840 Microbiol Rev *25*, 107-123.
841 Garay-Arroyo, A., and Covarrubias, A.A. (1999). Three genes whose expression is induced by
842 stress in Saccharomyces cerevisiae. Yeast *15*, 879-892.
843 Garreau, H., Hasan, R.N., Renault, G., Estruch, F., Boy-Marcotte, E., and Jacquet, M. (2000).
844 Hyperphosphorylation of Msn2p and Msn4p in response to heat shock and the diauxic shift is
845 inhibited by cAMP in Saccharomyces cerevisiae. Microbiol. *146*, 2113-2120.
846 Gietz, R.D., Schiestl, R.H., Willems, A.R., and Woods, R.A. (1995). Studies on the
847 transformation of intact yeast cells by the LiAc/SS- DNA/PEG procedure. Yeast *11*, 355-360.
848 Gorner, W., Durchschlag, E., Martinez-Pastor, M.T., Estruch, F., Ammerer, G., Hamilton, B.,
849 Ruis, H., and Schuller, C. (1998). Nuclear localization of the C2H2 zinc finger protein Msn2p is
850 regulated by stress and protein kinase A activity. Genes Dev *12*, 586-597.
851 Griffioen, G., Anghileri, P., Imre, E., Baroni, M.D., and Ruis, H. (2000). Nutritional control of
852 nucleocytoplasmic localization of cAMP-dependent protein kinase catalytic and regulatory
853 subunits in Saccharomyces cerevisiae. J. Biol. Chem. *275*, 1449-1456.
854 Griffioen, G., Laan, R.J., Mager, W.H., and Planta, R.J. (1996). Ribosomal protein gene
855 transcription in *Saccharomyces cerevisiae* shows a biphasic response to nutritional changes.
856 Microbiol. *142*, 2279-2287.
857 Griffioen, G., Mager, W.H., and Planta, R.J. (1994). Nutritional upshift response of ribosomal
858 protein gene transcription in *Saccharomyces cerevisiae.* FEMS Microbiol. Lett. *123*, 137-144.
859 Heinemeyer, T., Wingender, E., Reuter, I., Hermjakob, H., Kel, A.E., Kel, O.V., Ignatieva, E.V.,
860 Ananko, E.A., Podkolodnaya, O.A., Kolpakov, F.A., Podkolodny, N.L., and Kolchanov, N.A.
861 (1998). Databases on transcriptional regulation: TRANSFAC, TRRD and COMPEL. Nucleic
862 Acids Res *26*, 362-367.
863 Hughes, J.D., Estep, P.W., Tavazoie, S., and Church, G.M. (2000). Computational identification
864 of cis-regulatory elements associated with groups of functionally related genes in Saccharomyces
865 cerevisiae. J Mol Biol *296*, 1205-1214.
866 Iyengar, R. (1996). Gating by cyclic AMP: expanded role for an old signaling pathway. Science
867 *271*, 461-463.
868 Jang, Y.K., Wang, L., and Sancar, G.B. (1999). RPH1 and GIS1 are damage-responsive
869 repressors of PHR1. Mol Cell Biol *19*, 7630-7638.
870 Jiang, Y., Davis, C., and Broach, J.R. (1998). Efficient transition to growth on fermentable
871 carbon sources in *Saccharomyces cerevisiae* requires signaling through the Ras pathway. EMBO
872 J. *17*, 6942-6951.
873 Jordan, J.D., and Iyengar, R. (1998). Modes of interactions between signaling pathways. Biochem
874 Pharmacol *55*, 1347-1352.
875 Jorgensen, P., Nishikawa, J.L., Breitkreutz, B.J., and Tyers, M. (2002). Systematic identification
876 of pathways that couple cell growth and division in yeast. Science *297*, 395-400.
877 Kirchner, J., Sanders, S.L., Klebanow, E., and Weil, P.A. (2001). Molecular genetic dissection of
878 TAF25, an essential yeast gene encoding a subunit shared by TFIID and SAGA multiprotein
879 transcription factors. Mol Cell Biol *21*, 6668-6680.

880 Klein, C., and Struhl, K. (1994). Protein kinase A mediates growth-regulated expression of yeast
881 ribosomal protein genes by modulating RAP1 transcriptional activity. Mol. Cell. Biol. *14*, 1920-
882 1928.
883 Kurdistani, S.K., Robyr, D., Tavazoie, S., and Grunstein, M. (2002). Genome-wide binding map
884 of the histone deacetylase Rpd3 in yeast. Nat Genet *31*, 248-254.
885 Laloux, I., Jacobs, E., and Dubois, E. (1994). Involvement of SRE element of Ty1 transposon in
886 TEC1-dependent transcriptional activation. Nucleic Acids Res *22*, 999-1005.
887 Lee, H., Rezai-Zadeh, N., and Seto, E. (2004). Negative regulation of histone deacetylase 8
888 activity by cyclic AMP-dependent protein kinase A. Mol Cell Biol *24*, 765-773.
889 Lenssen, E., Oberholzer, U., Labarre, J., De Virgilio, C., and Collart, M.A. (2002).
890 Saccharomyces cerevisiae Ccr4-not complex contributes to the control of Msn2p-dependent
891 transcription by the Ras/cAMP pathway. Mol Microbiol *43*, 1023-1037.
892 Lorenz, M.C., Pan, X., Harashima, T., Cardenas, M.E., Xue, Y., Hirsch, J.P., and Heitman, J.
893 (2000). The G protein-coupled receptor Gpr1 is a nutrient sensor that regulates pseudohyphal
894 differentiation in *Saccharomyces cerevisiae*. Genetics *154*, 609-622.
895 Ma, P., Wera, S., Van Dijck, P., and Thevelein, J.M. (1999). The PDE1-encoded low-affinity
896 phosphodiesterase in the yeast Saccharomyces cerevisiae has a specific function in controlling
897 agonist- induced cAMP signaling. Mol Biol Cell *10*, 91-104.
898 Mager, W.H., and De Kruijff, A.J. (1995). Stress-induced transcriptional activation. Microbiol
899 Rev *59*, 506-531.
900 Marchler, G., Schuller, C., Adam, G., and Ruis, H. (1993). A Saccharomyces cerevisiae UAS
901 element controlled by protein kinase A activates transcription in response to a variety of stress
902 conditions. Embo J *12*, 1997-2003.
903 Martinez-Pastor, M.T., Marchler, G., Schuller, C., Marchler-Bauer, A., Ruis, H., and Estruch, F.
904 (1996). The Saccharomyces cerevisiae zinc finger proteins Msn2p and Msn4p are required for
905 transcriptional induction through the stress response element (STRE). Embo J *15*, 2227-2235.
906 Mayordomo, I., Estruch, F., and Sanz, P. (2002). Convergence of the target of rapamycin and the
907 Snf1 protein kinase pathways in the regulation of the subcellular localization of Msn2, a
908 transcriptional activator of STRE (Stress Response Element)-regulated genes. J. Biol. Chem. *277*,
909 35650-35656.
910 Mbonyi, K., Beullens, M., Detremerie, K., Geerts, L., and Thevelein, J.M. (1988). Requirement
911 of one functional RAS gene and inability of an oncogenic ras variant to mediate the glucose-
912 induced cyclic AMP signal in the yeast Saccharomyces cerevisiae. Mol Cell Biol *8*, 3051-3057.
913 Mitsuzawa, H. (1993). Responsiveness to exogenous cAMP of a saccharomyces cerevisiae strain
914 conferred by naturally occurring alleles of PDE1 and PDE2. Genetics *135*, 321-326.
915 Morano, K.A., and Thiele, D.J. (1999). The Sch9 protein kinase regulates Hsp90 chaperone
916 complex signal transduction activity in vivo. Embo J *18*, 5953-5962.
917 Mösch, H-U., Kübler, E., Krappmann, S., Fink, G.R., and Braus, G.H. (1999) Crosstalk between
918 the Ras2p-controlled mitogen-activated protein kinase and cAMP pathways during invasive
919 growth of *Saccharomyces cerevisiae*. Mol. Biol. Cell *10*, 1325-1335
920 Moskvina, E., Schuller, C., Maurer, C.T., Mager, W.H., and Ruis, H. (1998). A search in the
921 genome of Saccharomyces cerevisiae for genes regulated via stress response elements. Yeast *14*,
922 1041-1050.
923 Myers, A.M., Tzagoloff, A., Kinney, D.M., and Lusty, C.J. (1986). Yeast shuttle and integrative
924 vectors with multiple cloning sites suitable for construction of lacZ fusions. Gene *45*, 299-310.
925 Nikawa, J., Cameron, S., Toda, T., Ferguson, K.M., and Wigler, M. (1987a). Rigorous feedback
926 control of cAMP levels in Saccharomyces cerevisiae. Genes Dev *1*, 931-937.

Nikawa, J., Sass, P., and Wigler, M. (1987b). Cloning and characterization of the low-affinity cyclic AMP phosphodiesterase gene of *Saccharomyces cerevisiae*. Mol. Cell. Biol. *7*, 3629-3636.
Ortiz, C.H., Maia, J.C., Tenan, M.N., Braz-Padrao, G.R., Mattoon, J.R., and Panek, A.D. (1983). Regulation of yeast trehalase by a monocyclic, cyclic AMP-dependent phosphorylation-dephosphorylation cascade system. J. Bacteriol. *153*, 644-651.
Pedruzzi, I., Burckert, N., Egger, P., and De Virgilio, C. (2000). Saccharomyces cerevisiae Ras/cAMP pathway controls post-diauxic shift element-dependent transcription through the zinc finger protein Gis1. EMBO J. *19*, 2569-2579.
Pedruzzi, I., Dubouloz, F., Cameroni, E., Wanke, V., Roosen, J., Winderickx, J., and De Virgilio, C. (2003). TOR and PKA signaling pathways converge on the protein kinase Rim15 to control entry into G0. Mol Cell *12*, 1607-1613.
Pnueli, L., Edry, I., Cohen, M., and Kassir, Y. (2004). Glucose and nitrogen regulate the switch from histone deacetylation to acetylation for expression of early meiosis-specific genes in budding yeast. Mol Cell Biol *24*, 5197-5208.
Reinders, A., Burckert, N., Boller, T., Wiemken, A., and De Virgilio, C. (1998). *Saccharomyces cerevisiae* cAMP-dependent protein kinase controls entry into stationary phase through the Rim15p protein kinase. Genes Dev *12*, 2943-2955.
Rohde, J.R., and Cardenas, M.E. (2003). The tor pathway regulates gene expression by linking nutrient sensing to histone acetylation. Mol Cell Biol *23*, 629-635.
Ruis, H., and Schuller, C. (1995). Stress signaling in yeast. Bioessays *17*, 959-965.
Schmelzle, T., Beck, T., Martin, D.E., and Hall, M.N. (2004). Activation of the RAS/cyclic AMP pathway suppresses a TOR deficiency in yeast. Mol Cell Biol *24*, 338-351.
Sherman, F., Fink, G.R., and Hicks, J.B. (1986). Methods in yeast genetics. Cold Spring Harbor Laboratory Press: Cold Spring Harbor.
Smith, A., Ward, M.P., and Garrett, S. (1998). Yeast PKA represses Msn2p/Msn4p-dependent gene expression to regulate growth, stress response and glycogen accumulation. EMBO J. *17*, 3556-3564.
Tavazoie, S., Hughes, J.D., Campbell, M.J., Cho, R.J., and Church, G.M. (1999). Systematic determination of genetic network architecture. Nat Genet *22*, 281-285.
Thevelein, J.M., and Beullens, M. (1985). Cyclic AMP and the stimulation of trehalase activity in the yeast *Saccharomyces cerevisiae* by carbon sources, nitrogen sources and inhibitors of protein synthesis. J. Gen. Microbiol. *131*, 3199-3209.
Thevelein, J.M., Cauwenberg, L., Colombo, S., De Winde, J.H., Donation, M., Dumortier, F., Kraakman, L., Lemaire, K., Ma, P., Nauwelaers, D., Rolland, F., Teunissen, A., Van Dijck, P., Versele, M., Wera, S., and Winderickx, J. (2000). Nutrient-induced signal transduction through the protein kinase A pathway and its role in the control of metabolism, stress resistance, and growth in yeast. Enzyme Microb Technol *26*, 819-825.
Thevelein, J.M., and de Winde, J.H. (1999). Novel sensing mechanisms and targets for the cAMP - protein kinase A pathway in the yeast *Saccharomyces cerevisiae*. Mol. Microbiol. *32*, 1002-1012.
Thijs, G., Marchal, K., Lescot, M., Rombauts, S., De Moor, B., Rouze, P., and Moreau, Y. (2002). A gibbs sampling method to detect overrepresented motifs in the upstream regions of coexpressed genes. J Comput Biol *9*, 447-464.
Thomas, B.J., and Rothstein, R.J. (1989). Elevated recombination rates in transcriptionally active DNA. Cell *56*, 619-630.

Toda, T., Cameron, S., Sass, P., and Wigler, M. (1988). *SCH9*, a gene of *Saccharomyces cerevisiae* that encodes a protein distinct from, but functionally and structurally related to cAMP-dependent protein kinase catalytic subunits. Gene Dev. *2*, 517-527.

Toda, T., Cameron, S., Sass, P., Zoller, M., Scott, J.D., McMullen, B., Hurwitz, M., Krebs, E.G., and Wigler, M. (1987a). Cloning and characterization of BCY1, a locus encoding a regulatory subunit of the cyclic AMP-dependent protein kinase in Saccharomyces cerevisiae. Mol Cell Biol *7*, 1371-1377.

Toda, T., Cameron, S., Sass, P., Zoller, M., and Wigler, M. (1987b). Three different genes in *Saccharomyces cerevisiae* encode the catalytic subunits of the cAMP-dependent protein kinase. Cell *50*, 277-287.

Uno, I., Matsumoto, K., Adachi, K., and Ishikawa, T. (1983). Genetic and biochemical evidence that trehalase is a substrate of cAMP-dependent protein kinase in yeast. J. Biol. Chem. *258*, 10867-10872.

van Helden, J., Andre, B., and Collado-Vides, J. (2000). A web site for the computational analysis of yeast regulatory sequences. Yeast *16*, 177-187.

Wang, Y., Pierce, M., Schneper, L., Guldal, C.G., Zhang, X., Tavazoie, S., and Broach, J.R. (2004). Ras and gpa2 mediate one branch of a redundant glucose signaling pathway in yeast. PLoS Biol *2*, E128.

Werner-Washburne, M., Braun, E., Johnston, G.C., and Singer, R.A. (1993). Stationary phase in the yeast *Saccharomyces cerevisiae*. Microbiol. Rev. *57*, 383-401.

Wilson, R.B., Renault, G., Jacquet, M., and Tatchell, K. (1993). The pde2 gene of Saccharomyces cerevisiae is allelic to rca1 and encodes a phosphodiesterase which protects the cell from extracellular cAMP. FEBS Lett. *325*, 191-195.

Wilson, R.B., and Tatchell, K. (1988). SRA5 encodes the low-Km cyclic AMP phosphodiesterase of Saccharomyces cerevisiae. Mol Cell Biol *8*, 505-510.

Winderickx, J., de Winde, J.H., Crauwels, M., Hino, A., Hohmann, S., Van Dijck, P., and Thevelein, J.M. (1996). Regulation of genes encoding subunits of the trehalose synthase complex in *Saccharomyces cerevisiae*: novel variations of STRE-mediated transcription control ? Mol. Gen. Genet. *252*, 470-482.

Zahringer, H., Holzer, H., and Nwaka, S. (1998). Stability of neutral trehalase during heat stress in Saccharomyces cerevisiae is dependent on the activity of the catalytic subunits of cAMP-dependent protein kinase, Tpk1 and Tpk2. Eur. J. Biochem. *255*, 544-551.

Zhu, H., Klemic, J.F., Chang, S., Bertone, P., Casamayor, A., Klemic, K.G., Smith, D., Gerstein, M., Reed, M.A., and Snyder, M. (2000). Analysis of yeast protein kinases using protein chips. Nat Genet *26*, 283-289.

Figure Legends

Figure 1: PKA and Sch9 define separate signalling cascades. A) Growth of mutant strains in the absence and presence of 3 mM cAMP on rich glucose or glycerol/ethanol containing medium. B) Summary figure of the parallel and converging effector branches of the PKA and Sch9 signalling pathways. C) PKA and Sch9 requirement for proper glucose-induced trehalase activation. Strains *pde2Δ cyr1Δ msn2Δ msn4Δ* (Δ,▲), *pde2Δ cyr1Δ msn2Δ msn4Δ sch9Δ* (◊,♦) and *pde2Δ cyr1Δ msn2Δ msn4Δ* YIp*SCH9* (□,■) with (open symbols) or without (closed symbols) pre-treatment of 0.5 mM cAMP were supplemented with 100mM glucose at time 0 to induce activation of trehalase. Average values over 3 independent measurements are shown with an average standard deviation of 2.19.

Figure 2: Genome-wide expression profiling of normalized intensities using the AQBC clustering algorithm. A) Genes were clustered based on their normalized intensities in the strains (1) *pde2Δ cyr1Δ msn2Δ msn4Δ*, (2) *pde2Δ cyr1Δ msn2Δ msn4Δ sch9Δ* and (3) *pde2Δ cyr1Δ msn2Δ msn4Δ* YIp*SCH9* grown in the absence (a) or in the presence (b) of 3mM cAMP. Output of AQBC clustering - normalized intensity profiles of the genes - is shown (black lines). For each cluster, the mean expression profile is also shown (bold gray line). NOG = Number Of Genes assigned to each cluster. Chart axes are shown in the empty chart on the lower right side. B) Schematic representation for each class depicting the effect on expression in the different strains under conditions with and without 3 mM cAMP. Filled lines represent the effects of PKA and Sch9 when considered separately (2a versus 2b and 1a versus 2a respectively) while dashed lines represent the combined effects of both kinases (1a versus 1b and 1b versus 2b). The most highly enriched MIPS functional categories for each class are shown.

Figure 3: ***In vivo*** **confirmation of the mathematical predictions by REDUCE.** Beta-galactosidase assays in the strains indicated using promoter reporter constructs pJS205XN1B, pJS205XN4B, pJS205XN3B containing one single element of the DNA-elements A) TGAAAAA (RRPE), B) AAACG (U4) or C) TAAGG (PDS) respectively. Values are represented as actual specific activity (nmoles min^{-1} mg $protein^{-1}$) with baseline zero representing the background activity of the empty vector. Averages of three independent measurements are shown.

Figure 4: Sch9 positively regulates PDS-driven gene expression. A) Northern blot analysis of typical PDS (*GRE1, SSA3*) and STRE (*HSP12*, *DDR2)* genes upon shift from glucose- to glycerol-containing rich medium in various mutants. *18S* is used as a reference. Samples were taken at the indicated time points. B) Nucleocytoplasmic localization of Gis1-GFP and Msn2-GFP is not affected by Rim15 or Sch9. Localization was visualized either with or without addition of 1µg/ml DAPI in the absence or presence of 100 nM rapamycin. Images represent at least 3 independent observations. C) Growth on glycerol-containing medium of mutants affected in the activities of Sch9, Rim15, Msn2/4 and/or Gis1.

Figure 5: Sch9 and TOR signalling are subject to cAMP-gating in yeast. Model for cAMP-gating effect in yeast consisting of a main gatekeeper, the protein kinase PKA, switching on or off the activities and signals transmitted through primary pathways such as Sch9 and TOR. Sch9 positively controls PDS-driven gene expression mainly via Gis1 and Rim15. TOR and PKA control STRE-driven gene expression mainly via Msn2/4 and Rim15. GTF stands for general transcription complex. Note that the effect of PKA on Msn2/4 localization is not depicted here. Arrows and bars refer to positive and negative interactions. Dashed lines refer to potential cross-regulation. See text for details.

Supplementary data

Figure S1: Cyclic AMP-dependency for growth. A) Growth of mutant strains in the absence and presence of 3 mM cAMP on glucose or glycerol/ethanol containing medium on minimal synthetic complete medium. B) Alleviation of the growth defect of the *pde2Δ cyr1Δ msn2Δ msn4Δ sch9* mutant strain. Growth can only be restored by reintroduction of *SCH9*, not by overexpression of *TPK1* or *BCY1*.

Figure S2: Northern Blot analysis of randomly selected genes confirmed the genome-wide expression profiles. Strains (1) *pde2Δ cyr1Δ msn2Δ msn4Δ*, (2) *pde2Δ cyr1Δ msn2Δ msn4Δ sch9Δ*, (3) *pde2Δ cyr1Δ msn2Δ msn4Δ* YIp*SCH9* and (4) W303-1A in the absence (a) or in the presence (b) of 3mM cAMP. Quantitative expression values are shown relative to actine (*ACT1*) as a control.

Table 1: PKA and Sch9 specific target genes

ORF	Gene	effect of cAMP[a]		effect of *SCH9*[a]		Biological function
		SCH9[b]	*sch9*Δ[b]	-cAMP[b]	+cAMP[b]	
PKA Specific (11 genes)						
Induced						
YGR103W	*NOP7*	**2,86**	**2,15**	1,01	1,34	nucleolar protein
YGR160W	*FYV13*	**2,52**	**3,00**	1,39	1,16	hypothetical protein
YJL033W	*HCA4*	**2,88**	**2,18**	1,17	1,54	RNA helicase CA4
YKL044W		**2,15**	**3,01**	1,02	-1,37	hypothetical protein
YLR089C		**2,41**	**2,51**	1,31	1,26	putative alanine aminotransferase
YMR290C	*HAS1*	**3,41**	**2,17**	-1,20	1,31	RNA helicase
Repressed						
YBR072W	*HSP26*	**-6,13**	**-4,07**	1,49	-1,01	heat shock protein
YDR155C	*CPH1*	**-3,69**	**-2,86**	1,05	-1,23	cyclophilin (peptidylprolyl isomerase)
YGR144W	*THI4*	**-2,82**	**-2,42**	-1,17	-1,37	thiamine repressed protein
YHL035C		**-2,18**	**-2,41**	1,10	1,21	transporter activity
YIR036C		**-2,32**	**-2,58**	1,22	1,36	reductase
Sch9 Specific (24 genes)						
Induced						
YBR218C	*PYC2*	1,15	1,25	**2,48**	**2,27**	pyruvate carboxylase 2
YBR249C	*ARO4*	1,23	1,39	**3,07**	**2,72**	2-dehydro-3-deoxyphosphoheptonate aldolase
YDL081C	*RPP1A*	1,31	1,38	**2,66**	**2,52**	acidic ribosomal protein P1A
YDR046C	*BAP3*	1,26	1,21	**2,34**	**2,45**	branched chain amino acid permease
YDR399W	*HPT1*	1,30	1,03	**2,19**	**2,76**	hypoxanthine phosphoribosyl transferase
YEL046C	*GLY1*	1,39	1,11	**2,76**	**3,45**	L-threonine aldolase, low-specific
YER091C	*MET6*	-1,26	-1,23	**2,46**	**2,39**	methionine synthase
YFR030W	*MET10*	-1,36	-1,06	**3,77**	**2,93**	sulfite reductase flavin-binding subunit
YGR124W	*ASN2*	1,13	1,43	**2,99**	**2,36**	asparagine synthetase
YGR240C	*PFK1*	1,08	1,40	**3,26**	**2,51**	6-phosphofructokinase, alpha subunit
YGR271W	*SLH1*	1,42	1,25	**2,43**	**2,77**	SKI2-like helicase'
YJL008C	*CCT8*	-1,20	1,46	**4,00**	**2,28**	component of TCP ring complex
YJL101C	*GSH1*	-1,46	-1,42	**3,04**	**2,94**	gamma glutamylcysteine synthetase
YJR010W	*MET3*	1,19	-1,24	**2,95**	**4,37**	sulfate adenylyltransferase
YKL054C	*DEF1*	1,35	1,29	**2,49**	**2,60**	RNA PolII degradation factor 1
YKL148C	*SDH1*	-1,46	-1,43	**3,10**	**3,03**	succinate dehydrogenase flavoprotein subunit
YLR130C	*ZRT2*	-1,02	-1,18	**2,49**	**2,87**	low affininty zinc transporter
YLR302C		1,22	1,06	**6,76**	**7,77**	protein of unknown function
YLR303W	*MET17*	1,04	1,32	**6,01**	**4,73**	O-acetylhomoserine sulfhydrylase
YML002W		-1,34	-1,32	**2,67**	**2,62**	hypothetical protein
YML123C	*PHO84*	1,10	1,02	**4,27**	**4,59**	high-affinity inorganic phosphate symporter
YMR108W	*ILV2*	-1,20	1,38	**4,26**	**2,57**	acetolacetate synthase
Repressed						
YFR026C		1,30	1,29	**-2,11**	**-2,09**	protein of unknown function
YIL058W		1,16	-1,27	**-3,32**	**-2,25**	protein of unknown function

[a] variable parameter: Effect of cAMP or presence of *SCH9* in the strain *pde2*Δ *cyr1*Δ *msn2/4*Δ. Values represent fold change difference in expression. See text and experimental procedures for selection procedures.

[b] constant parameter

Genes were deemed PKA specific when their fold changes difference in expression exceeded 2 due to addition of cAMP in both strains and when the fold change difference in expression did not exceed 1.5 due to the presence of *SCH9*.

Genes were deemed Sch9 specific when their fold change difference in expression exceeded 2 due to the presence of *SCH9* and when the fold change difference in expression did not exceed 1.5 due to addition of cAMP.

Table 2: Cis-acting promoter elements identified by REDUCE (R) and/or Motif Finder (M)

Method	Element	Name	Consensus Sequence	Transcription Factor	Cluster[a]	PKA correlation[b]	Sch9 correlation[b]
R/M	AGGGG	STRE	AG4	Msn2/4	4,5,6,9,14	-	0
R	GATGAG	PAC	AKCTCATCKC	Unknown	1,7	+	0
R	(C)(C)(T/A)AAGG(G)	PDS	TWAG3AT	Gis1	4,5,6	-	+
R/M	(C)ACCCAT(A)	RPG	RMACCANNCAYY	Rap1	1,10,13	+	+
R	TGAAAAA	RRPE	WGAAAAAWWTT	Unknown	1	+	+
R	AAAATTT(T)	RRPE	AAAATTT	Unknown	1	+	+
M	TGAAAC	PRE	A/TGAACA	Ste12	7,8,9	ND[c]	ND[c]
M	CATTCT	FRE	CATTCC/T	Tec1	7,8,9	ND[c]	ND[c]
R	CCG repeat	URS1	TAGCCGCCGA	Ime1/Ume6	1,13	0	+
R	(T)CCGTAC(A)	U1	Unknown	Unknown	1,14	+	+
R	(G)(V)CTGG(A)(C)	U2	Unknown	Unknown	1,4,14	-	+
R	CAGGCCG	U3	Unknown	Unknown	1,7,11,13	+	+
R	AAACG	U4	Unknown	Unknown	1	0	+
R	GGATTCC	U5	Unknown	Unknown	7,12	+	-

[a] The distribution for each element in each cluster relative to its genome-wide distribution was calculated according to Tavazoie *et al.*, 1999. Elements were deemed significantly enriched when the minus log2(p-values) exceeded 1.

[b] + = positive correlation; - = negative correlation; 0 = no correlation. The PKA and/or Sch9 correlation was determined based on the F(Multi)-scores of the tested DNA motif in a given comparison as calculated by REDUCE (Bussemaker *et al.*, 2001). F(Multi)-score: the contribution of the identified DNA motif to the log2ratio of gene Ag relative to the baseline level C according the formula $Ag = C + \Sigma F*N$. Negative values correspond to a drop in expression whereas positive values correspond to higher expression as function of a particular DNA-motif.

[c] not detected by REDUCE.

Table 3: PKA and Sch9 oppositely regulate STRE/PDS-driven gene expression.

ORF	Gene	cAMP[a]	*SCH9*[b]	Biological function	STRE	PDS
Stress Response						
YDR353W	*TRR1*	-13,71	4,82	thioredoxin reductase	0	1
YDR513W	*TTR1*	-4,69	3,73	glutaredoxin	2	1
YER103W	*SSA4*	-4,33	5,11	heat shock protein	3	3
YFL014W	*HSP12*	-7,74	6,92	heat shock protein	7	3
YGR088W	*CTT1*	-9,11	5,05	cytosolic catalase T	4	4
YHR008C	*SOD2*	-6,52	5,63	manganese superoxide dismutase	1	1
YJR104C	*SOD1*	-4,22	4,88	copper-zinc superoxide dismutase	1	2
YLL026W	*HSP104*	-10,18	4,53	heat shock protein	3	2
YLL060C	*GTT2*	-5,32	4,30	glutathione transferase	0	1
YML028W	*TSA1*	-4,59	3,33	thioredoxin peroxidase	1	1
YML070W	*DAK1*	-8,49	6,68	dihydroxyacetone kinase	0	3
YMR096W	*SNZ1*	-3,38	3,80	putative pyridoxin	0	1
YMR175W	*SIP18*	-5,96	3,82	'Salt-induced protein'	3	1
YNL160W	*YGP1*	-6,56	3,87	'Yeast Glycoprotein'	2	0
YOL053C-A	*DDR2*	-9,89	3,96	DNA-damage responsive'	4	3
YOR027W	*STI1*	-4,53	3,34	'Stress Inducible'	0	2
YPL223C	*GRE1*	-7,82	8,66	stress responsive gene	0	4
YPL240C	*HSP82*	-5,37	3,03	heat shock protein	2	0
Energy						
YCL040W	*GLK1*	-3,25	3,98	glucokinase	3	0
YDR074W	*TPS2*	-3,18	3,35	trehalose-6-phosphate phosphatase	5	2
YER178W	*PDA1*	-4,01	3,04	pyruvate dehydrogenase, α-subunit	2	1
YFL056C	*AAD6*	-6,05	6,56	aryl alcohol dehydrogenase	0	0
YGR087C	*PDC6*	-6,96	6,77	pyruvate decarboxylase isoenzyme 3	0	2
YGR256W	*GND2*	-9,17	3,60	6-phosphogluconate dehydrogenase	2	1
YML100W	*TSL1*	-3,64	3,33	tre-6-P synthase complex, regulatory subunit	3	1
YNL241C	*ZWF1*	-3,65	5,29	glucose-6-P dehydrogenase	5	3
Metabolism						
YAL062W	*GDH3*	-6,64	3,46	glutamate dehydrogenase	0	0
YBR026C	*ETR1*	-7,29	4,40	2-enoyl thioester reductase	1	2
YDR368W	*YPR1*	-6,22	3,25	2-methylbutyraldehyde reductase	0	0
YHR037W	*PUT2*	-3,34	3,35	P5C dehydrogenase	0	1
YKL157W	*APE2*	-6,90	6,06	aminopeptidase 2	0	1
YOL058W	*ARG1*	-3,30	3,31	argininosuccinate synthetase	2	2
YOL151W	*GRE2*	-4,93	5,53	α-acetoxy ketone reductase	0	4
YOR374W	*ALD4*	-5,37	3,81	mitochondrial aldehyde dehydrogenase	2	0
Other						
YBR008C	*FLR1*	-8,40	6,96	fluconazole resistance protein'	1	2
YDL126C	*CDC48*	-4,75	4,67	component of ERAD system	1	1
YHR139C	*SPS100*	-7,43	4,63	sporulation specific protein	3	8
YJL056C	*ZAP1*	-3,70	3,30	zinc-responsive transcriptional activator	0	1
YKR076W	*ECM4*	-12,28	7,16	Extracellular Mutant'	2	1
YPL036W	*PMA2*	-9,45	6,98	P-type ATPase	4	3

[a] genes repressed by addition of cAMP in the strain *pde2*Δ *cyr1*Δ *msn2/4*Δ

[b] genes induced by *SCH9* in the strain *pde2*Δ *cyr1*Δ *msn2/4*Δ in the absence of cAMP

Only genes with a known function and of which the fold change difference in expression exceeded 3 across both comparisons (a and b) were retained (See Exp. Proced. for details on data normalization and analysis). The number of STRE (AG4) and PDS (TAAGG) elements within 1000 base pairs (bp) upstream of the transcription start sites (non-coding sequences only) of the corresponding ORFs is indicated (overlapping matches were allowed).

Table 4: Strains used in this study

Strain	Genotype	Reference
W303-1A	*MATa ade2-1 can1-100 his3-11,15 leu2-3,112 trp1-1 ura3-1*	Thomas and Rothstein, 1989
Wmsn2msn4	*MATa* W303 with *msn2-3::HIS3 msn4-1::TRP1*	Martinez-Pastor *et al.*, 1996
CDV115	*MATa* W303 with *rim15::KanMX2*	Pedruzzi *et al.*, 2003
CDV122	*MATa* W303 with *gis1::KanMX2*	Pedruzzi *et al.*, 2003
CDV124	*MATa* Wmsn2msn4 with *gis1::KanMX2*	Pedruzzi *et al.*, 2003
TVH301	*MATa* W303 with *sch9::TRP1*	this study
BD7	*MATα* W303 with *sch9::TRP1*	this study
BD2	*MATa* Wmsn2msn4 with *rim15::KanMX2*	this study
BD3	*MATa* seggregant of Wmsn2msn4 and BD7	this study
BD9	*MATa* seggregant of BD2 and BD3	this study
BD13	*MATa* CDV124 with *sch9::LEU2*	this study
GG103	*MATa* W303 with *pde2::TRP1 cdc35::KanMX2*	this study
GG104	*MATa* GG103 with *msn2::HIS3 msn4::TRP1*	this study
ASY62	*MATa tpk1::ADE8 tpk2::HIS3 tpk3::TRP1 msn2::HIS3 msn4::LEU2*	Smith *et al.*, 1998
RJ_100A	*MATa* GG104 with *sch9::URA3*	this study
RJ_100B	*MATa* GG104 with *sch9::LEU2*	this study
RJ_101	*MATa* GG103 with YIp*SCH9*	this study
RJ_102	*MATa* GG104 with YIp*SCH9*	this study
RJ_201	*MATa* CDV115 with *sch9::LEU2*	Pedruzzi *et al.*, 2003
RJ_202	*MATa* CDV122 with *sch9::LEU2*	this study

Figure R1

A

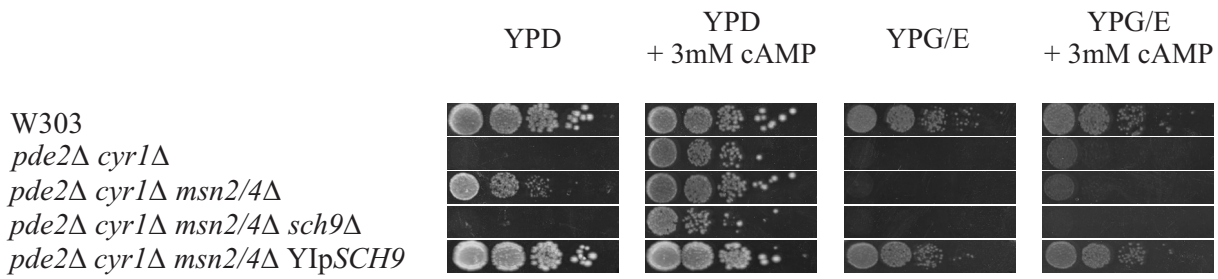

B

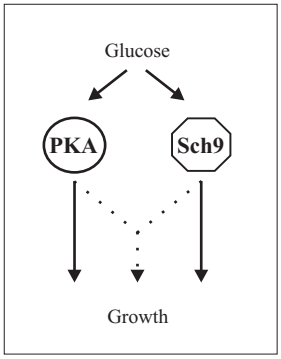

C

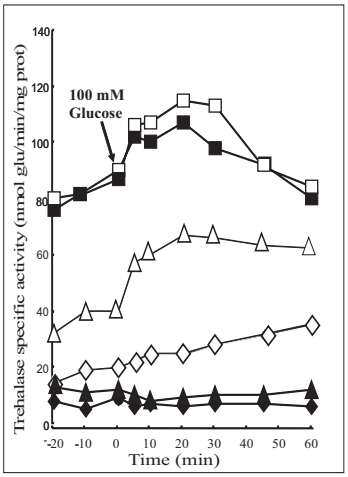

Figure 2

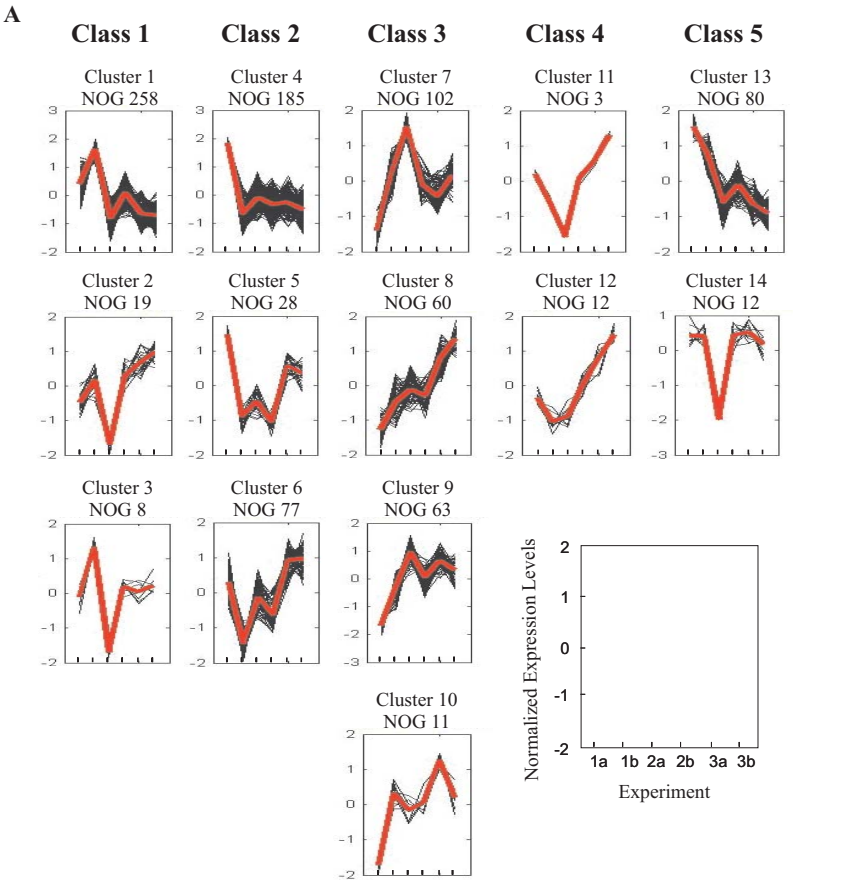
A
Class 1
Class 2
Class 3
Class 4
Class 5
Cluster 1
NOG 258
Cluster 4
NOG 185
Cluster 7
NOG 102
Cluster 11
NOG 3
Cluster 13
NOG 80
Cluster 2
NOG 19
Cluster 5
NOG 28
Cluster 8
NOG 60
Cluster 12
NOG 12
Cluster 14
NOG 12
Cluster 3
NOG 8
Cluster 6
NOG 77
Cluster 9
NOG 63
Cluster 10
NOG 11
Normalized Expression Levels
1a 1b 2a 2b 3a 3b
Experiment

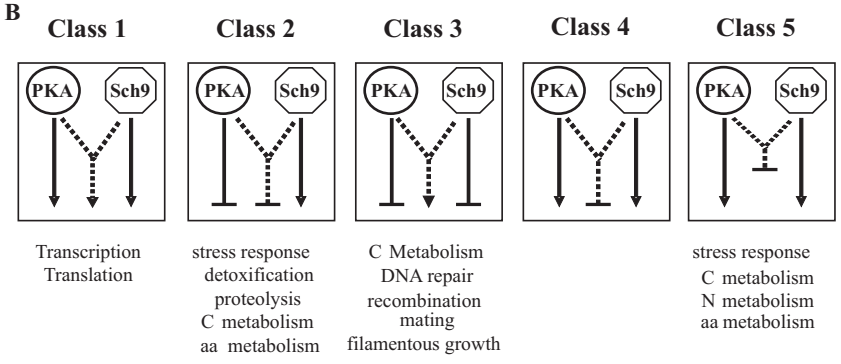
B
Class 1
Class 2
Class 3
Class 4
Class 5
PKA
Sch9
Transcription
Translation
stress response
detoxification
proteolysis
C metabolism
aa metabolism
C Metabolism
DNA repair
recombination
mating
filamentous growth
stress response
C metabolism
N metabolism
aa metabolism

Figure 3

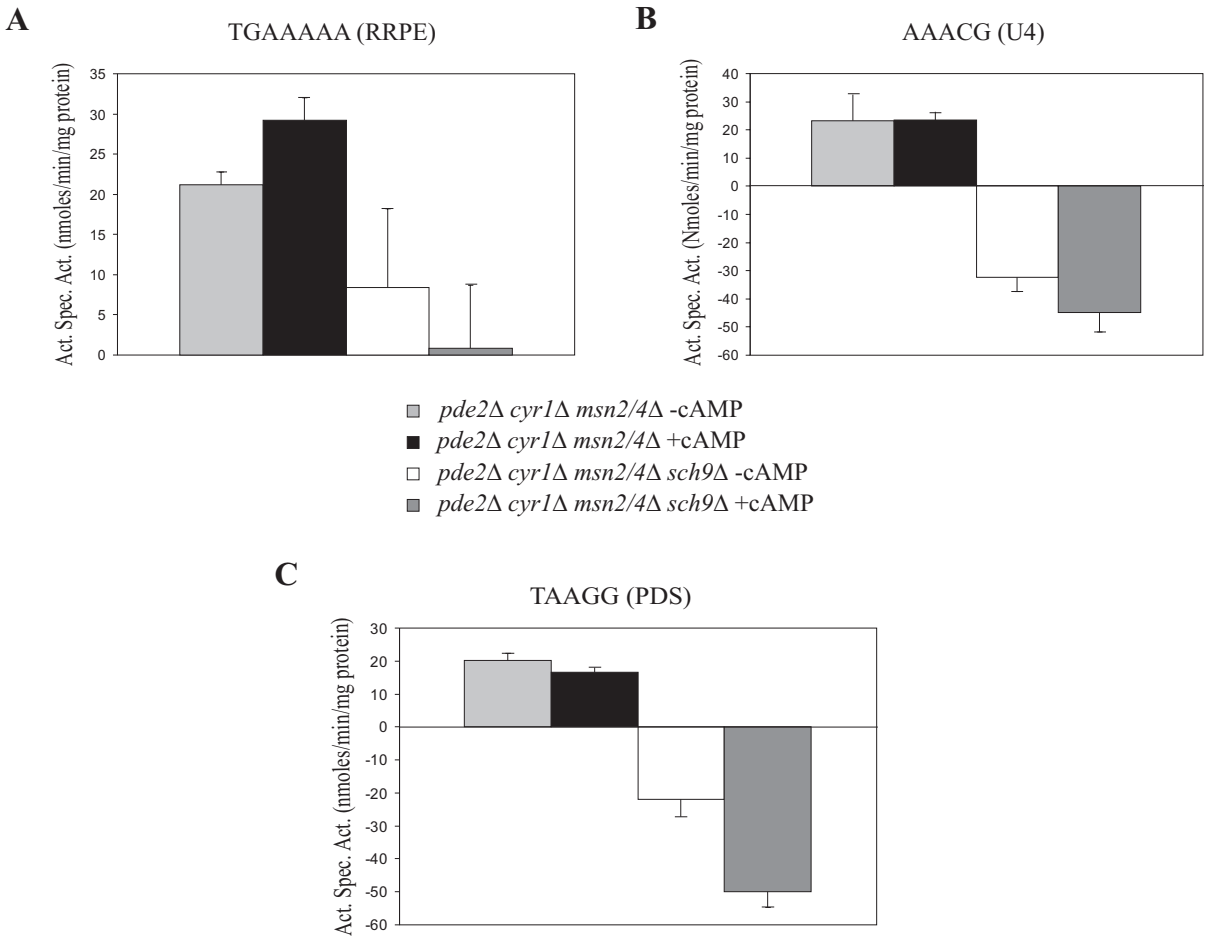
A
TGAAAAA (RRPE)
Act. Spec. Act. (nmoles/min/mg protein)
35
30
25
20
15
10
5
0
B
AAACG (U4)
Act. Spec. Act. (Nmoles/min/mg protein)
40
30
20
10
0
-10
-20
-30
-40
-50
-60
pde2Δ cyr1Δ msn2/4Δ -cAMP
pde2Δ cyr1Δ msn2/4Δ +cAMP
pde2Δ cyr1Δ msn2/4Δ sch9Δ -cAMP
pde2Δ cyr1Δ msn2/4Δ sch9Δ +cAMP
C
TAAGG (PDS)
Act. Spec. Act. (nmoles/min/mg protein)
30
20
10
0
-10
-20
-30
-40
-50
-60

Figure 4

A

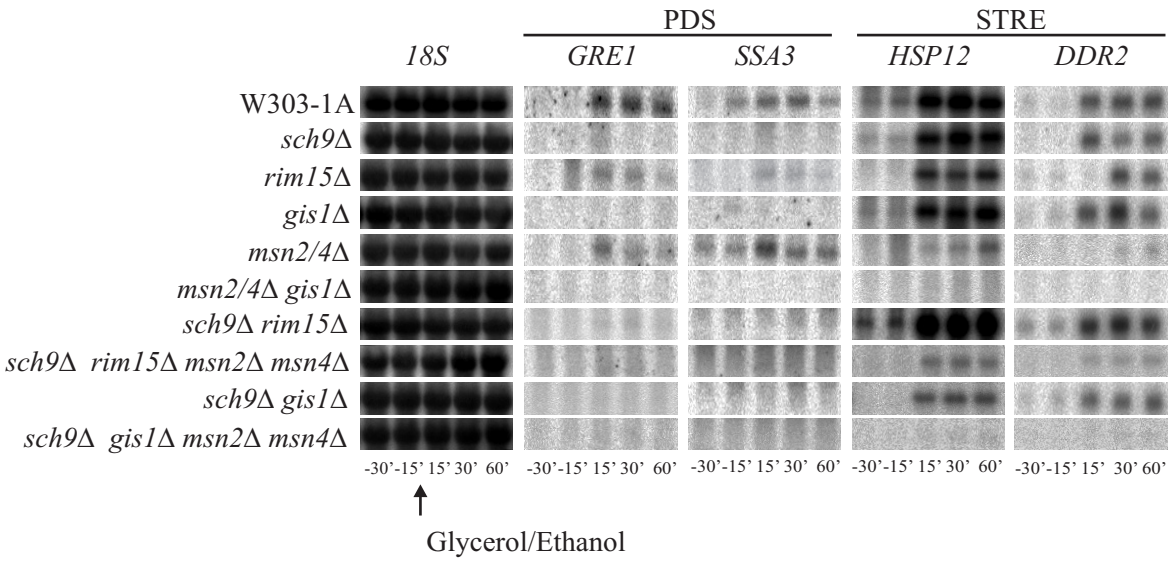
PDS
STRE
18S
GRE1
SSA3
HSP12
DDR2
W303-1A
sch9Δ
rim15Δ
gis1Δ
msn2/4Δ
msn2/4Δ gis1Δ
sch9Δ rim15Δ
sch9Δ rim15Δ msn2Δ msn4Δ
sch9Δ gis1Δ
sch9Δ gis1Δ msn2Δ msn4Δ
-30'-15' 15' 30' 60'
Glycerol/Ethanol

B

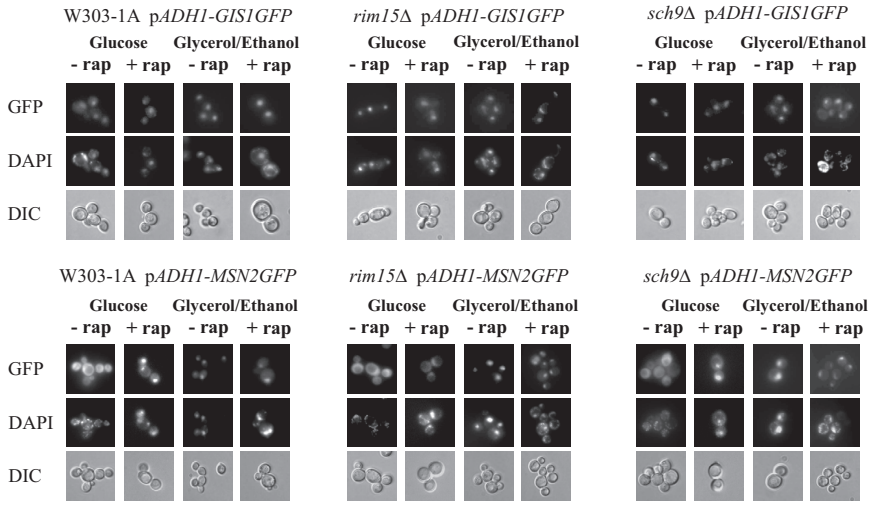
W303-1A pADH1-GIS1GFP
rim15Δ pADH1-GIS1GFP
sch9Δ pADH1-GIS1GFP
Glucose
Glycerol/Ethanol
- rap
+ rap
GFP
DAPI
DIC
W303-1A pADH1-MSN2GFP
rim15Δ pADH1-MSN2GFP
sch9Δ pADH1-MSN2GFP

C

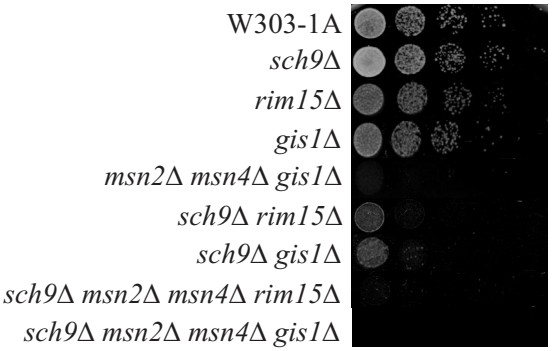
W303-1A
sch9Δ
rim15Δ
gis1Δ
msn2Δ msn4Δ gis1Δ
sch9Δ rim15Δ
sch9Δ gis1Δ
sch9Δ msn2Δ msn4Δ rim15Δ
sch9Δ msn2Δ msn4Δ gis1Δ

Figure R5

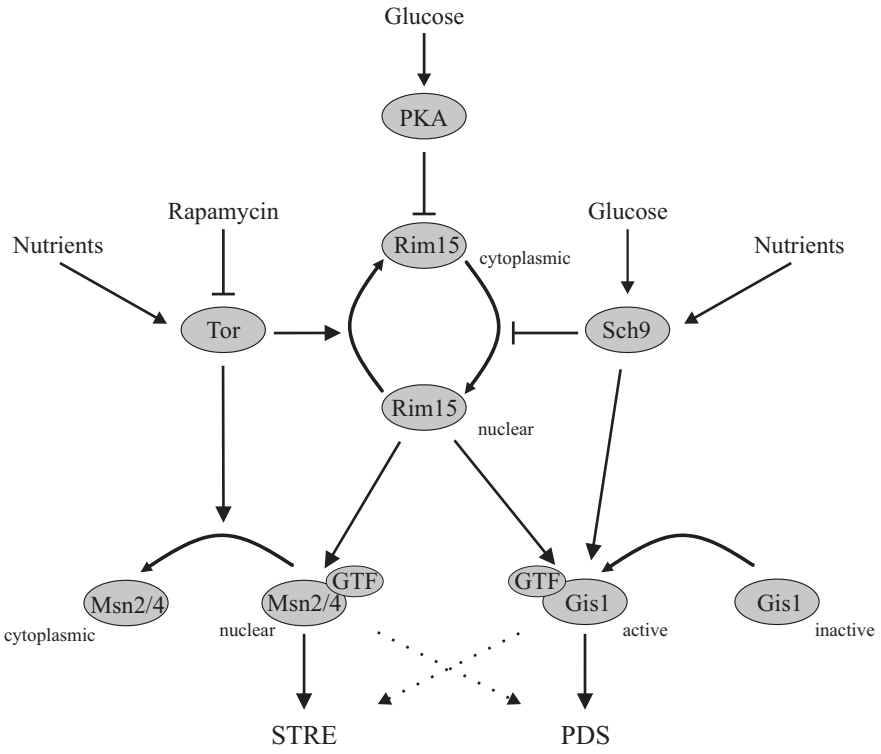
Glucose
PKA
Rapamycin
Glucose
Nutrients
Rim15
cytoplasmic
Nutrients
Tor
Sch9
Rim15
nuclear
GTF
GTF
Msn2/4
Msn2/4
Gis1
Gis1
cytoplasmic
nuclear
active
inactive
STRE
PDS

Supplementary data

Table S1: The strain *pde2*Δ *cyr1*Δ *msn2/4*Δ exhibits a normal transcriptional cAMP response

ORF	Gene	cAMP[a]	Biological process (MIPS)	Reference
Induced by cAMP				
YGL147C	*RPL9A*	4,11	ribosome biogenesis	Griffioen *et al.*, 1994; Klein and Struhl, 1994
YGL031C	*RPL24A*	2,63	ribosome biogenesis	Griffioen *et al.*, 1994; Klein and Struhl, 1994
YLR340W	*RPP0*	2,79	ribosome biogenesis	Griffioen *et al.*, 1994; Klein and Struhl, 1994
YLL045C	*RPL8B*	3,66	ribosome biogenesis	Griffioen *et al.*, 1994; Klein and Struhl, 1994
YHR010W	*RPL27A*	3,19	ribosome biogenesis	Griffioen *et al.*, 1994; Klein and Struhl, 1994
YGR148C	*RPL24B*	3,15	ribosome biogenesis	Griffioen *et al.*, 1994; Klein and Struhl, 1994
YIL018W	*RPL2B*	2,45	ribosome biogenesis	Griffioen *et al.*, 1994; Klein and Struhl, 1994
YOR234C	*RPL33B*	3,49	ribosome biogenesis	Griffioen *et al.*, 1994; Klein and Struhl, 1994
YBL027W	*RPL19B*	2,20	ribosome biogenesis	Griffioen *et al.*, 1994; Klein and Struhl, 1994
YHL033C	*RPL8A*	2,55	ribosome biogenesis	Griffioen *et al.*, 1994; Klein and Struhl, 1994
YIL133C	*RPL16A*	2,00	ribosome biogenesis	Griffioen *et al.*, 1994; Klein and Struhl, 1994
YKL006W	*RPL14A*	2,60	ribosome biogenesis	Griffioen *et al.*, 1994; Klein and Struhl, 1994
YKL180W	*RPL17A*	2,70	ribosome biogenesis	Griffioen *et al.*, 1994; Klein and Struhl, 1994
YOL127W	*RPL25*	3,52	ribosome biogenesis	Griffioen *et al.*, 1994; Klein and Struhl, 1994
YJL189W	*RPL39*	2,07	ribosome biogenesis	Griffioen *et al.*, 1994; Klein and Struhl, 1994
YGR085C	*RPL11*B	2,14	ribosome biogenesis	Griffioen *et al.*, 1994; Klein and Struhl, 1994
YBR084C-A	*RPL19A*	2,15	ribosome biogenesis	Griffioen *et al.*, 1994; Klein and Struhl, 1994
Repressed by cAMP				
YGR088W	*CTT1*	-9,11	stress response	Marchler *et al*., 1993; Winderickx *et al*., 1996
YFL014W	*HSP12*	-7,74	stress response	Varela *et al.*, 1995; Donalis and Stahl, 2001
YLL026W	*HSP104*	-10,18	stress response	Boy-Marcotte *et al.*, 1998; Donalis and Stahl, 2001
YCR021C	*HSP30*	-7,12	stress response	Puig and Perez-Ortin, 2000; Donalis and Stahl, 2001
YBR072W	*HSP26*	-6,13	stress response	Amoros and Estruch, 2001; Donalis and Stahl, 2001
YAL062W	*GDH3*	-6,64	amino acid degradation	Boy-Marcotte *et al.*, 1998
YOL126C	*MDH2*	-6,35	glyoxylate cycle	Tadi *et al*., 1998
YGR019W	*UGA1*	-6,30	amino acid biosynthesis	Tadi *et al.*, 1998
YBL075C	*SSA3*	-3,46	stress response	Winderickx *et al.*, 1996; Boy-Marcotte *et al.*, 1998
YHR008C	*SOD2*	-6,52	detoxification	Flattery-O'Brien *et al*., 1997; Boy-Marcotte *et al.*, 1998
YDR171W	*HSP42*	-7,12	protein folding	Moskvina *et al.*, 1998; Donalis and Stahl, 2001
YDR258C	*HSP78*	-3,64	stress response	Moskvina *et al.*, 1998; Donalis and Stahl, 2001
YML100W	*TSL1*	-3,64	energy reserve metabolism	Winderickx *et al*., 1996
YDL022W	*GPD1*	-6,21	carbohydrate metabolism	Boy-Marcotte *et al*., 1998
YBR006W	*UGA2*	-4,72	amino acid degradation	Tadi *et al*., 1998
YKL157W	*APE2*	-6,90	amino acid metabolism	Tadi *et al*., 1998
YMR169C	*ALD3*	-2,52	fermentation	Boy-Marcotte *et al*., 1998
YHR033W		-2,60	amino acid biosynthesis	Tadi *et al*., 1998
YBR286W	*APE3*	-3,50	proteolytic degradation	Tadi *et al.*, 1998
YBR126C	*TPS1*	-3,04	carbohydrate metabolism	Winderickx *et al.*, 1996; Boy-Marcotte *et al.*, 1998

[a] Strains were grown exponentially on YPgalactose in the absence or presence of 3mM cAMP. Only genes of which the average fold change difference in expression exceeded 2 were deemed significantly. Positive values refer to induction of gene expression by addition of cAMP, negative values refer to repression of gene expression by addition of cAMP.

Table S2: Expected frequency of occurence.

	AGGGG	GATGAG	TAAGGG	ACCCAT	TGAAAAA	AAAATTT	CCGCCG	CCGTAC	CTGG	CAGGCCG	AAACG	GGATTCC
Cluster 1	0.6	**4.7**	0.0	**10.3**	**10.4**	**24.2**	**1.2**	**7.1**	**3.7**	**2.9**	**2.2**	0.5
Cluster 2	0.0	0.4	0.2	0.1	0.0	0.2	0.1	0.1	0.1	0.0	0.0	0.0
Cluster 3	0.0	0.0	0.1	0.5	0.1	0.5	0.3	0.7	0.2	0.0	0.4	0.0
Cluster 4	**8.2**	0.3	**9.3**	0.5	0.0	0.0	0.4	0.9	**2.3**	0.4	0.5	0.8
Cluster 5	**2.7**	0.1	**1.0**	0.4	0.2	0.0	0.4	0.6	0.2	0.0	0.1	0.7
Cluster 6	**2.2**	0.5	**1.6**	0.3	0.0	0.0	0.9	0.2	0.9	0.0	0.5	0.0
Cluster 7	0.0	**2.0**	0.1	0.6	0.1	0.1	0.2	0.5	0.1	**1.4**	0.4	**1.4**
Cluster 8	0.0	0.3	0.1	0.1	0.2	0.0	0.2	0.0	0.0	0.0	0.3	0.1
Cluster 9	**1.1**	0.0	0.3	0.7	0.0	0.0	0.0	0.1	0.3	0.0	0.3	0.2
Cluster 10	0.3	0.2	0.0	**1.2**	0.7	0.0	0.0	0.5	0.7	0.0	0.4	0.5
Cluster 11	0.1	0.2	0.3	0.0	0.1	0.1	0.7	0.0	0.1	**1.3**	0.6	0.0
Cluster 12	0.5	0.9	0.2	0.3	0.4	0.2	0.2	0.2	0.4	0.0	0.1	**2.3**
Cluster 13	0.4	0.0	0.9	**1.0**	0.8	0.3	**2.1**	0.0	0.4	**6.2**	0.1	0.0
Cluster 14	**2.3**	0.2	0.2	0.6	0.9	0.6	0.2	**1.0**	**1.6**	0.0	0.5	0.0
Class 1	0.2	**4.5**	0.0	**9.5**	**8.6**	**22.4**	**1.1**	**6.7**	**3.2**	**2.5**	**1.6**	0.3
Class 2	**11.6**	0.4	**10.4**	0.5	0.0	0.0	0.9	0.8	**2.5**	0.1	0.4	0.6
Class 3	0.1	0.3	0.1	**1.0**	0.0	0.0	0.1	0.1	0.1	0.3	0.5	0.9
Class 4	0.5	0.9	0.3	0.2	0.3	0.2	0.5	0.1	0.3	0.7	0.2	**2.0**
Class 5	**1.1**	0.0	0.9	**1.2**	**1.1**	0.4	**2.0**	0.1	0.8	**5.6**	0.1	0.0

The distribution for each element in each cluster relative to its genome-wide distribution was calculated according to Tavazoie *et al.*, 1999. Minus log2(p-values) are shown. A cut-off value of 1 was applied to select statistically overrepresented motifs in a particular class (highlighted in bold). 1000 basepairs (bp) upstream of the transcription start sites of the ORFs in each class (non-coding sequences only) were scanned for the presence of at least one particular DNA motif using RSA tools (overlapping matches were allowed).

Figure S1

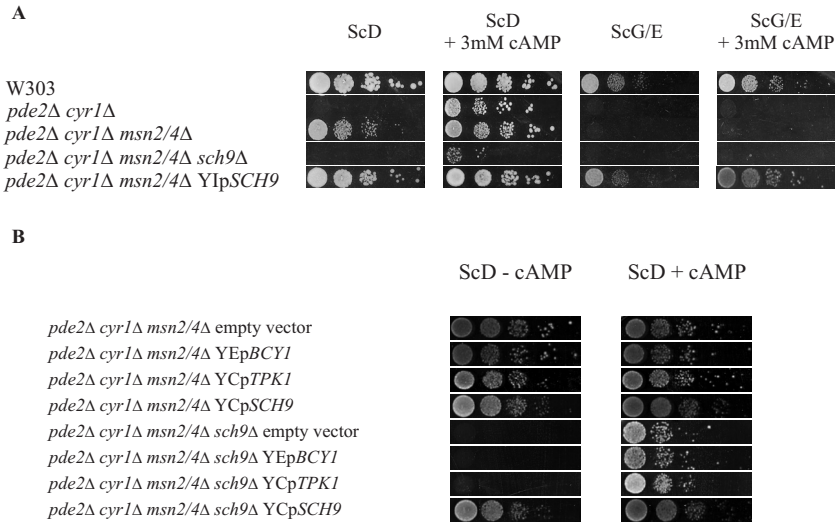
A
ScD
ScD
+ 3mM cAMP
ScG/E
ScG/E
+ 3mM cAMP
W303
pde2Δ cyr1Δ
pde2Δ cyr1Δ msn2/4Δ
pde2Δ cyr1Δ msn2/4Δ sch9Δ
pde2Δ cyr1Δ msn2/4Δ YIpSCH9
B
ScD - cAMP
ScD + cAMP
pde2Δ cyr1Δ msn2/4Δ empty vector
pde2Δ cyr1Δ msn2/4Δ YEpBCY1
pde2Δ cyr1Δ msn2/4Δ YCpTPK1
pde2Δ cyr1Δ msn2/4Δ YCpSCH9
pde2Δ cyr1Δ msn2/4Δ sch9Δ empty vector
pde2Δ cyr1Δ msn2/4Δ sch9Δ YEpBCY1
pde2Δ cyr1Δ msn2/4Δ sch9Δ YCpTPK1
pde2Δ cyr1Δ msn2/4Δ sch9Δ YCpSCH9

Figure S2

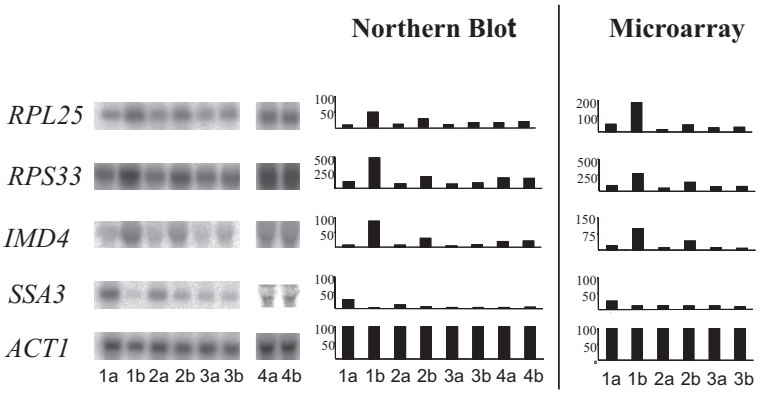
Northern Blot
Microarray
RPL25
RPS33
IMD4
SSA3
ACT1
1a 1b 2a 2b 3a 3b 4a 4b
1a 1b 2a 2b 3a 3b 4a 4b
1a 1b 2a 2b 3a 3b

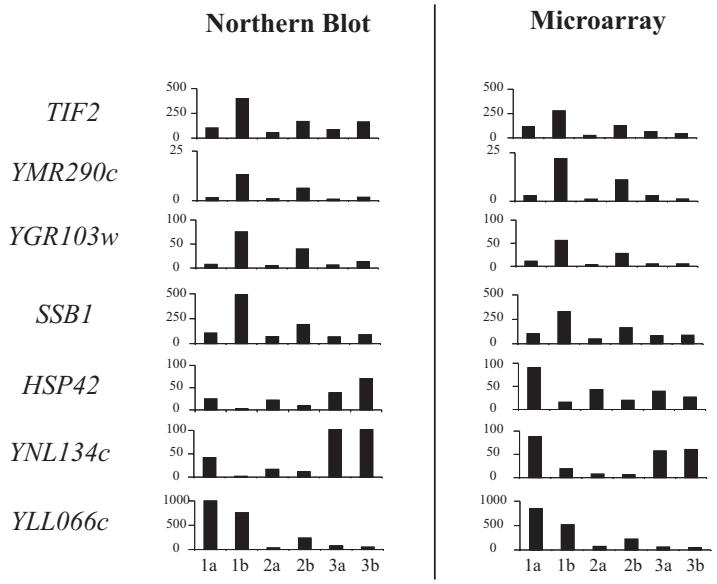
Northern Blot
Microarray
TIF2
YMR290c
YGR103w
SSB1
HSP42
YNL134c
YLL066c
1a 1b 2a 2b 3a 3b
1a 1b 2a 2b 3a 3b